JACS
JOURNAL OF THE AMERICAN CHEMICAL SOCIETY
Article
pubs.acs.org/JACS

Understanding the Reactivity of Strained Sandwich Compounds with Aluminum or Gallium in Bridging Positions: Experiments and DFT Calculations

Bidraha Bagh,[†] Gabriele Schatte,[‡] Jennifer C. Green,[§] and Jens Müller*[,†]

[†]Department of Chemistry and [‡]Saskatchewan Structural Sciences Centre, University of Saskatchewan, 110 Science Place, Saskatoon, Saskatchewan S7N 5C9, Canada

[§]Department of Chemistry, Inorganic Chemistry Laboratory, University of Oxford, Oxford OX1 3QR, United Kingdom

Supporting Information

ABSTRACT: The aluminum and gallium dichlorides (Mamx)-ECl_2 **1a** (*E* = Al; 82%) and **1b** (E = Ga; 79%) (Mamx = 2,4-di-*tert*-butyl-6-[(dimethylamino)methyl]phenyl) reacted with dilithioferrocene or dilithioruthenocene to give [1]ferrocenophanes (**2a**, **2b**) and [1]ruthenocenophanes (**3a**, **3b**), respectively. The galla[1]ruthenocenophane **3b** could be isolated from the reaction mixture through precipitation into hexane (50%), while **2a**, **2b**, and **3a** underwent ring-opening polymerization under the reaction conditions of their formation reactions to give metallopolymers (M_w (DLS) between 8.07 and 106 kDa). Monomer **3b** was polymerized using Karstedt's catalyst resulting in an M_w of 28.6(±6.3) kDa. In order to get an indication of the structure of polymers, bis(ferrocenyl) compounds (Mamx)EFc_2 (E = Al (**4a**), 51%; E = Ga (**4b**), 49%) were prepared and characterized by single crystal X-ray analysis. DFT calculations shed some light on the unexpected high reactivity of these new strained sandwich species. Optimized geometries of known aluminum and gallium-bridged [1]ferrocenophanes (Al(Pytsi) (**6a**), Ga(Pytsi) (**6b**); Pytsi = [dimethyl(2-pyridyl)silyl]bis(trimethylsilyl)methyl) and [1]ruthenocenophanes (Al(Me_2Ntsi) (**7a**), Ga(Me_2Ntsi) (**7b**); Me_2Ntsi = [(dimethylamino)dimethylsilyl]bis(trimethylsilyl)methyl) matched very well with experimental molecular structures. Geometries of species **2a**, **2b**, **3a**, and **3b** were optimized (BP86/TZ2P) and the structural influence of the *t*Bu group of the Mamx ligand in ortho position was evaluated by optimizing molecular structures of the four unknown species where the *ortho*-*t*Bu group was replaced by an H atom (**2a**^{H}, **2b**^{H}, **3a**^{H}, and **3b**^{H}). The most pronounced structural effect was seen as a change of the orientation of the bridging moiety with respect to the sandwich unit. As the *t*Bu group was removed, the aromatic ligand moved toward the freed-up space. The energetics (ΔE, ΔH^{298K}, and ΔG^{298K}) accompanied by the structural changes were evaluated by a hydrogenolysis reaction of strained species resulting in Cp_2M (*M* = Fe, Ru) and respective aluminum and gallium dihydrides. This nonisodesmic reaction showed that [1]metallocenophanes equipped with the *ortho*-*t*Bu group were on average 5.5 kcal/mol higher strained (ΔH^{298K}) than species where the *t*Bu group was lacking. The investigation of the isodesmic reaction between strained species and Cp_2M yielding bis(metallocenyl) compounds revealed that the *ortho*-*t*Bu group sterically interacts with one of the metallocenyl units. The bis(metallocenyl) compounds are model compounds for the respective metallopolymers and one can conclude that even though the *ortho*-*t*Bu group imposes additional strain on the starting metallocenophanes, this effect cancels out in ROPs because the *ortho*-*t*Bu group imposes a similar strain on the resulting polymers. The uncovered steric repulsion between the *ortho*-*t*Bu group and the sandwich moieties probably causes the *ortho*-*t*Bu to act as an unusually sensitive NMR probe of the tacticity of the polymers.

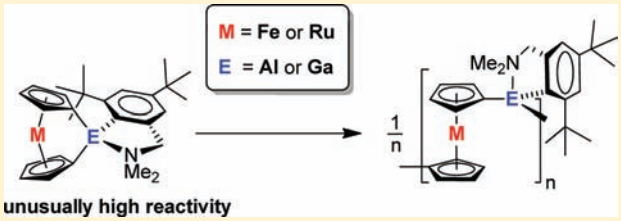

INTRODUCTION

In 1992, Manners et al. discovered that ring-opening polymerization (ROP) of sila[1]ferrocenophanes gives access to high-molecular-weight polymers.[1] Since this benchmark discovery, the synthesis of many new strained sandwich compounds has been reported.[2] In addition, different ROP methodologies were developed for the conversion of strained sandwich compounds into new metallopolymers,[3] a growing class of functional materials with high promise for applications in various areas.[3,4] Anionic-ROP of dimethylsila[1]ferrocenophane can be performed as a living polymerization, giving access to the important class of block copolymers.[5] These copolymers, with a poly(ferrocenylsilane) core (PFS; Chart 1), can form "living" micelles in block selective solvents; addition of further unimers results in larger micelles of uniform lengths. This new process was termed "crystallization-driven living self-assembly" and allows for controlled fabrication of uniform nanomaterials.[6]

Compared to the vast knowledge about PFS-based materials, that of respective group-13-containing polymers is still scarce. The most advanced class of group-13-containing polymers is that of boron,[7] and ferrocene-based materials had been

Received: February 27, 2012
Published: April 26, 2012

   dx.doi.org/10.1021/ja3019274 | J. Am. Chem. Soc. 2012, 134, 7924−7936

Chart 1. Poly(ferrocenyldimethylsilane), [1]Ferrocenophanes, and [1.1]Ferrocenophanes

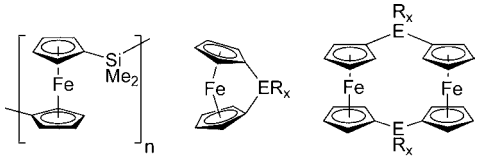

prepared by either ROP of bora[1]ferrocenophanes[8] or, more recently, through unusual redistribution/polycondensation reactions starting from 1,1′-bis(boryl)ferrocenes.[9] In order to develop poly(ferrocenyl) compounds of the heavier group 13 elements by ROP, we synthesized aluminum- and gallium-bridged sandwich compounds. After the preparation of the first aluminum- and gallium-bridged [1]ferrocenophanes (Chart 1) in 2005,[10a,b] [1]vanadarenophanes,[10c] [1]chromarenophanes,[10] [1]molybdarenophanes,[11] and [1]ruthenocenophanes[12] could be synthesized. All of these [1]metallacyclophanes were obtained by common salt metathesis reactions starting from dilithio-sandwich compounds and bulky dichlorides (Pytsi)ECl_2 or (Me_2Ntsi)ECl_2 (E = Al, Ga; Chart 2).

Chart 2

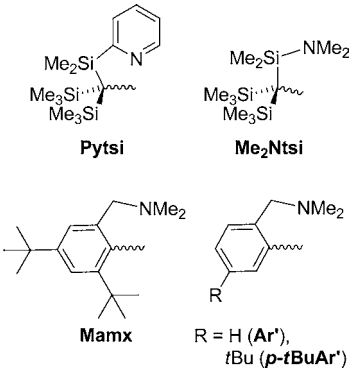

Unfortunately, attempts to polymerize by ring-opening aluminum- and gallium-bridged [1]ferrocenophanes and [1]-ruthenocenophanes either failed or resulted in sluggish reactions,[12] and it seemed that the bulkiness of the *trisyl*-type ligands Pytsi or Me_2Ntsi was hindering the ROP of those species. The bulkiness of the stabilizing ligand cannot easily be reduced: employing the less sterically encumbered ligands Ar′ or *p*-*t*BuAr′ (Chart 2) resulted in [1.1]metallacyclophanes[13] instead of the targeted [1]metallacyclophanes in respective salt metathesis reactions. Structural data of metallacyclophanes revealed that the bridging ER_x unit in [1.1]metallacyclophanes has less space available than in [1]metallacyclophanes.[14] On that basis, we speculated that, first, unstrained [1.1]-metallacyclophanes are thermodynamically preferred when starting compounds are equipped with the slim ligands Ar′ or *p*-*t*BuAr′ (Chart 2) and that, second, strained [1]-metallacyclophanes are obtained exclusively when the bulkiness of ligands hinders or even blocks the formation of [1.1]-metallacyclophanes. Therefore, we intended to use a ligand with just the right bulkiness to allow the formation of [1]metallacyclophanes but, at the same time, would not block their polymerizability. Our plan was to increase the bulkiness of the 2-[(dimethylamino)methyl]phenyl ligand (Ar′ in Chart 2) such that the formation of [1.1]ferrocenophanes, the outcome of salt metathesis reaction of Ar′ECl_2 (E = Al, Ga) with dilithioferrocene,[13a,b] would be impossible. From the known molecular structures of Ar′E-bridged [1.1]ferrocenophanes.[13a,b] It was evident that a *t*Bu group in the ortho position on the phenyl ring of the Ar′ ligand could not be accommodated. A ligand with these steric requirements was already known in form of the Mamx[15] ligand (Chart 2), which was introduced by Yoshifuji et al.[16] and had been used to stabilize phosphorus compounds.[17] Jutzi et al. employed the Mamx ligand to stabilize germanium species.[18]

In a recent short communication, we reported on the salt metathesis reaction of (Mamx)$GaCl_2$ with dilithioferrocene, which resulted in the formation of the targeted [1]-ferrocenophane **2b** (Scheme 1).[19] Unexpectedly, this strained

Scheme 1

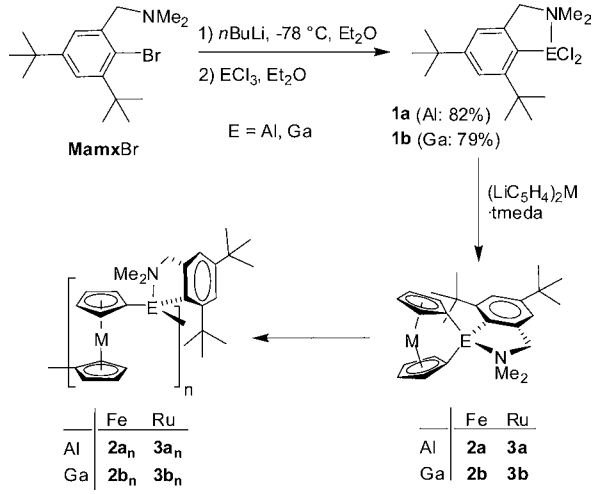

sandwich compound (**2b**) withstood all attempts at isolation and underwent ROP from reaction mixtures to give the poly(ferrocenylgallane) $\mathbf{2b_n}$ (Scheme 1). The *ortho*-*t*Bu group[20] acts as a very sensitive probe of the stereochemistry of the polymer backbone, and pentads were resolved in proton NMR spectra.[19] The splitting pattern of the *ortho*-*t*Bu group clearly revealed that polymer $\mathbf{2b_n}$ has a random tacticity. Here we report on the completed study of the reaction between (Mamx)ECl_2 (E = Al, Ga) and dilithioferrocene and dilithioruthenocene. New [1]ferrocenophanes and [1]-ruthenocenophanes and their respective metallopolymers are described. Using DFT calculations, we uncovered that the *ortho*-*t*Bu group significantly increases the strain in [1]-metallocenophanes, an unprecedented effect in metallocenophane chemistry.

RESULTS AND DISCUSSION

Synthesis of [1]Ferrocenophanes and [1]-Ruthenocenophanes. The aluminum and gallium dichlorides **1a** and **1b**,[19] respectively, are accessible in good yields starting from the bromide of the Mamx ligand following common methodologies (Scheme 1). As expected, NMR spectra of **1a** and **1b** are consistent with both species being C_s symmetric on the NMR time scale. That nitrogen is indeed coordinated to the group 13 element could be confirmed by a single crystal analysis of the gallium species **1b** (Figure 1 and Table 1), which showed a Ga−N bond length of 2.066(2) Å. As expected, the

dx.doi.org/10.1021/ja3019274 | J. Am. Chem. Soc. 2012, 134, 7924−7936

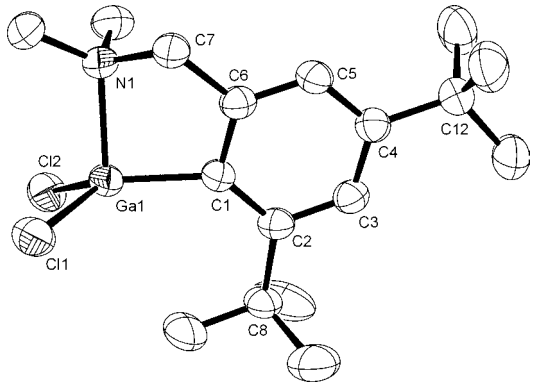

Figure 1. Molecular structure of **1b** with thermal ellipsoids at the 50% probability level. Hydrogen atoms and the solvent molecule C_7H_8 are omitted for clarity. Selected atom−atom distances [Å] and bond angles [°] for **1b**: Ga1−C1 = 1.956(2), Ga1−Cl1 = 2.1955(7), Ga1−Cl2 = 2.1878(7), Ga1−N1 = 2.066(2), C1−Ga1−Cl1 = 118.70(7), C1−Ga1−Cl2 = 125.94(7), C1−Ga1−N1 = 89.26(9), Cl1−Ga1−Cl2 = 108.51(3), N1−Ga1−Cl1 = 103.59(6), N1−Ga1−Cl2 = 104.40(7), Ga1−C1−C2 = 134.12(18), Ga1−C1−C6 = 106.88(17).

Table 1. Crystal and Structural Refinement Data for Compounds 1b, 4a, and 4b

	1b·C_7H_8	**4a·1/2C_6H_6**	**4b**
empirical formula	$C_{24}H_{36}Cl_2GaN$	$C_{40}H_{49}AlFe_2N$	$C_{37}H_{46}Fe_2GaN$
fw	479.19	682.50	686.17
cryst. size/mm^3	0.23 × 0.18 × 0.15	0.14 × 0.08 × 0.05	0.21 × 0.20 × 0.13
cryst. system, space group	monoclinic, $P2_1/c$	monoclinic, $P2_1/c$	triclinic, $P\bar{1}$
Z	4	4	2
a/Å	10.7202(5)	14.7365(3)	10.3706(3)
b/Å	17.6730(6)	10.9109(2)	11.7881(3)
c/Å	14.0352(5)	21.9806(5)	14.3895(3)
α/°	90	90	109.0902(7)
β/°	109.9730(10)	101.4210(10)	102.3199(8)
γ/°	90	90	97.1448(6)
volume/Å^3	2499.15(15)	3464.24(12)	1587.77(7)
ρ_{calc}/mg m^{-3}	1.273	1.309	1.435
temperature/K	173(2)	173(2)	173(2)
μ_{calc}/mm^{-1}	3.525	7.161	8.404
θ range/°	4.18 to 66.64	3.06 to 69.76	3.38 to 60.00
reflns collected/ unique	15167/4183	20971/6574	20043/4683
absorption correction	multiscan [SADABS]	multiscan [SADABS]	multiscan [SADABS]
data/restraints/ params	4183/15/262	6374/0/405	4683/0/378
goodness-of-fit	1.055	1.031	1.046
R_1 [I > 2 σ(I)][a]	0.0424	0.0660	0.0767
wR_2 (all data)[a]	0.1182	0.1799	0.1961
largest diff. peak and hole, $\Delta\rho_{elect}$/e Å^{-3}	0.725 and −0.555	1.458 and −0.409	1.450 and −1.248

[a] $R_1 = [\Sigma||F_o| - |F_c||]/[\Sigma|F_o|]$ for $[F_o^2 > 2\sigma(F_o^2)]$, $wR_2 = \{[\Sigma w(F_o^2 - F_c^2)^2]/[\Sigma w(F_o^2)^2]\}^{1/2}$ [all data].

molecular structure of **1b** did not reveal any surprises and is very similar to the known compounds 2-(Me_2NCH_2)-$C_6H_4GaCl_2$ and 2-(Me_2NCHMe)$C_6H_4GaCl_2$, which exhibit Ga−N bond lengths of 2.071(2)[21] and 2.049(3)[22] Å, respectively.

The dichlorides **1a** and **1b** were employed to prepare new aluminum- and gallium-bridged [1]ferrocenophanes (**2a**, **2b**[19]) and [1]ruthenocenophanes (**3a**, **3b**), starting from respective dilithio sandwich compounds (Scheme 1). Recently, we have shown that attempts to isolate the [1]ferrocenophane **2b** resulted in isolation of the polymer **2b**$_n$ (Scheme 1).[19] The respective aluminum compound **2a** shows a similar behavior and its isolation also gave polymers (**2a**$_n$). Proton NMR spectra taken from aliquots of reaction mixtures after 15−30 min clearly showed the presence of the strained [1]ferrocenophanes **2a** or **2b**, in particular by patterns and chemical shifts of the Cp protons, which are characteristic for alumina- or galla[1]-ferrocenophanes with donor-stabilizing ligands (C_s point-group symmetries).[10,12] This is illustrated in Figure 2, where the Cp

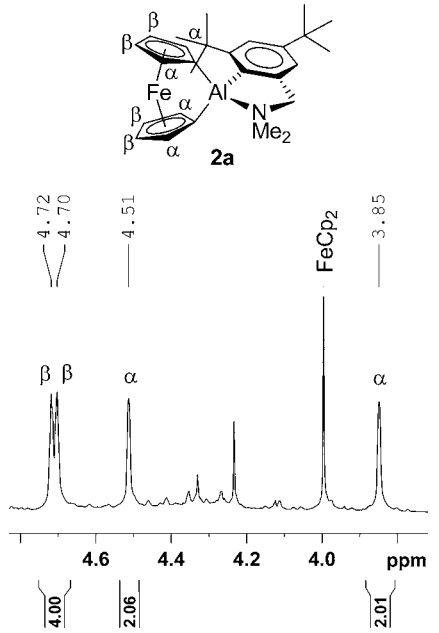

Figure 2. Cp range of the ^{1}H NMR spectrum of **2a** measured from an aliquot of the reaction mixture after ca. 30 min (C_6D_6).

range of the proton NMR spectrum of the aluminum compound **2a** is depicted. The two signals for the four H atoms in α-position to the bridging element are shifted upfield with respect to those of the four H atoms in β-potions [**2a**: δ 4.72 (2 β-H), 4.70 (2 β-H), 4.51 (2 α-H), 3.85 (2 α-H); **2b**: δ 4.69 (4 β-H), 4.56 (2 α-H), 4.01 (2 α-H)] (Figure 2 and S7 for **2a**; ref 19 for **2b**). In addition, the difference between the two signals of the α-protons is significantly larger than that of the β-protons.[23] Obviously, the influence of the disturbing bridging unit on α- compared to β-protons is distance dependent. Two chemically equivalent α-protons on one side of the [1]-ferrocenophane are in the neighborhood of the amine donor group, whereas the other pair of equivalent α-protons is on the opposite side of the sandwich (Figure 2). Because the β-protons are further away from the bridging moiety, they are not so sensitive toward the two different sides of the stabilizing ligand. In addition to the Cp protons, all expected signals were found for the [1]ferrocenophanes **2a** and **2b** (Figure S7 for **2a**; ref 19 for **2b**).

Judging by ^{1}H NMR spectra of reaction mixtures, the targeted species **2a** and **2b**, respectively, are the main products (e.g., Figure 2 and S7; ref 19 for **2b**). However, numerous attempts to isolate **2a** or **2b** through crystallization or precipitation into hexane failed (see the Experimental Section). Instead of the monomers **2a** and **2b**, the respective polymers

dx.doi.org/10.1021/ja3019274 | J. Am. Chem. Soc. 2012, 134, 7924−7936

$\mathbf{2a_n}$ and $\mathbf{2b_n}$ were isolated and further purified through precipitations into hexane and methanol, respectively, with isolated yields of 37% for $\mathbf{2a_n}$ and 45%[19] for $\mathbf{2b_n}$ (Scheme 1).

As shown in Scheme 1, the [1]ruthenocenophanes **3a** and **3b** were prepared using similar methods as were used for the [1]ferrocenophanes **2a** and **2b**. The aluminum-bridged [1]-ruthenocenophane **3a** showed a reactivity similar to that of the [1]ferrocenophanes **2a** and **2b**; however, the gallium-bridged [1]ruthenocenophane **3b** showed a lower reactivity and was isolated as a light yellow powder (50%) from filtered reaction mixtures through precipitation into hexane. Applying the same procedure to the aluminum species **3a** mainly gave polymers. Proton NMR spectra taken from the mother liquor after the precipitation into hexanes did not reveal significant amounts of the monomer **3a** showing that nearly all of the strained [1]ruthenocenophane **3a** polymerized to $\mathbf{3a_n}$ under these conditions. However, the reactivities of **3a** and **3b** are not vastly different. If reaction mixtures of the gallium species **3b** are left for 6 h, only its polymer $\mathbf{3b_n}$ could be isolated.

Attempts to grow crystals of **3b** for structural analysis failed (see the Experimental Section). However, ^{1}H NMR spectroscopy unequivocally revealed that strained [1]ruthenocenophanes **3a** and **3b** indeed formed in salt metathesis reactions of dichlorides and dilithioruthenocene (Scheme 1). Their Cp protons give similar patterns as those of the [1]-ferrocenophanes. For example, the two signals of the α-protons show the characteristic splitting that is significantly larger than that of the β-protons [**3a**: δ 5.34 (2 β-H), 5.30 (2 β-H), 4.65 (2 α-H), 4.02 (2 α-H); **3b**: δ 5.36 (2 β-H), 5.34 (2 β-H), 4.59 (2 α-H) 4.05 (2 α-H)] (Figure S10 and S13).

Metallopolymers. All four strained [1]metallocenophanes **2a**, **2b**, **3a**, and **3b** undergo ring-opening polymerizations (ROPs) at ambient temperature under the conditions of the salt metathesis reaction (Scheme 1). In addition, as we could isolate the monomer **3b**, ROPs using Karstedt's catalyst at ambient temperatures were performed (toluene, 5 mol % catalyst). All polymers were characterized by ^{1}H and ^{13}C NMR spectroscopy as well as by dynamic light scattering (DLS). Table 2 summarizes the results of the DLS analysis.

Table 2. DLS Analysis of Metallopolymers[a]

	R_h [nm]	M_w [kDa]	DP_w
$\mathbf{2a_n}$[c]	5.38 (±0.17)	106 (±8)	232 (±18)
$\mathbf{2b_n}$[b,c]	2.99 (±0.36)	36.0 (±8.4)	72 (±17)
$\mathbf{3a_n}$[c]	1.33 (±0.25)	8.07 (±3.0)	16 (±6)
$\mathbf{3b_n}$[c]	1.50 (±0.37)	10.1 (±4.8)	19 (±9)
$\mathbf{3b_n}$[d]	2.64 (±0.27)	28.6 (±6.3)	52 (±12)

[a]See also Tables S1−S5 and Figures S1−S4. [b]Data taken from ref 19. [c]Polymer from uncontrolled ROP. [d]Polymer from transition-metal-catalyzed ROP.

Assuming that the measured polymers were random coils in a good solvent, the radii of gyration can be calculated from the measured hydrodynamic radii (R_g/R_h = 2.05).[24] For poly(ferrocenyldimethylsilane) R_g and the absolute M_w are known,[25] which we employed to calculate the molecular weights shown in Table 2 (see the Experimental Section for details). The molecular weights of aluminum- and gallium-containing polymers vary between 8.07 and 106 kDa (Table 2). For the uncontrolled ROP, polyferrocenyl species $\mathbf{2a_n}$ and $\mathbf{2b_n}$ show significantly higher M_w values compared to those of their ruthenium analogues $\mathbf{3a_n}$ and $\mathbf{3b_n}$. The molecular weight of the polymer $\mathbf{3b_n}$ could be improved by using Karstedt's catalyst resulting in M_w values that were nearly three times as large compared to those of polymers obtained from the spontaneous, uncontrolled ROP (Table 2). For the gallium-containing polymer $\mathbf{2b_n}$, molecular weights were also determined with gel permeation chromatography (GPC) with polystyrene as a standard, resulting in 48 kDa for the sample that gave 36 kDa with respect to PFS as a standard by DLS analysis.[19]

Metallopolymers $\mathbf{2a_n}$, $\mathbf{2b_n}$, $\mathbf{3a_n}$, and $\mathbf{3b_n}$ are formed by ROP of the respective [1]metallocenophanes under the conditions of the metathesis formation reactions. So far, the mechanism of these ROPs is unknown, but it seems likely that some dilithioferrocene in reaction mixtures of the salt metathesis reaction acts as an anionic initiator (Scheme 1). Therefore, we wanted to test if addition of $ClSiMe_3$ to the reaction mixture influences the outcome of the ROP, and we investigated the reaction of the gallium dichloride **1b** with dilithioferrocene. Two parallel reactions were started in two different reaction vessels under the same reaction conditions, and after 15 min, excess Me_3SiCl was added to one reaction mixture. Both reactions were run for an additional 16 h followed by the work up as described for the synthesis of poly(ferrocenylgallane) $\mathbf{2b_n}$ (see ref 19). The polymers that resulted from the two reactions were identical with respect to ^{1}H NMR spectroscopy. The DLS analysis of the polymers gave similar hydrodynamic radii; R_h for the polymer of the reaction without Me_3SiCl was 3.31 nm and that with Me_3SiCl was 2.54 nm. The reaction in the presence of Me_3SiCl was done two additional times and gave identical polymers with respect to ^{1}H NMR spectroscopy. Comparison of polymers (with and without the addition of $ClSiMe_3$) did not reveal the presence of any Me_3Si end groups.

Bis(ferrocenyl) Species. In order to get an indication of the structure of polymers, the bis(ferrocenyl) compounds **4a** and **4b** have been prepared as they can be envisioned as small cutouts of the polymers $\mathbf{2a_n}$ and $\mathbf{2b_n}$, respectively. As illustrated in Scheme 2, both species were obtained by salt metathesis

Scheme 2

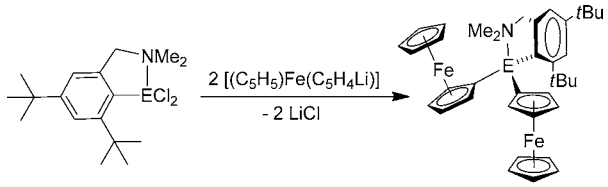

reactions starting from **1a** and **1b**, respectively, and isolated in moderate yields of 51% (**4a**) and 49% (**4b**).

Both species have been characterized by NMR spectroscopy, mass spectrometry, elemental analysis, and single crystal X-ray analysis (Table 1 and Figure 3 and 4).

Whereas the aluminum species **4a** (Figure 3) exhibits two ferrocenyl moieties oriented in approximately opposite directions, they are approximately parallel to each other in the gallium species **4b** (Figure 4). Both compounds show highly distorted tetrahedral coordination geometries around the group 13 element that are best described as trigonal-base pyramids with C1, C20, and C30 at the base and N1 at the tip. This description is justified as the sums over the three C−E−C (E = Al, Ga) angles with 352 (**4a**) and 359° (**4b**), respectively, are very close to 360°, indicating that the group 13 elements are

dx.doi.org/10.1021/ja3019274 | J. Am. Chem. Soc. 2012, 134, 7924−7936

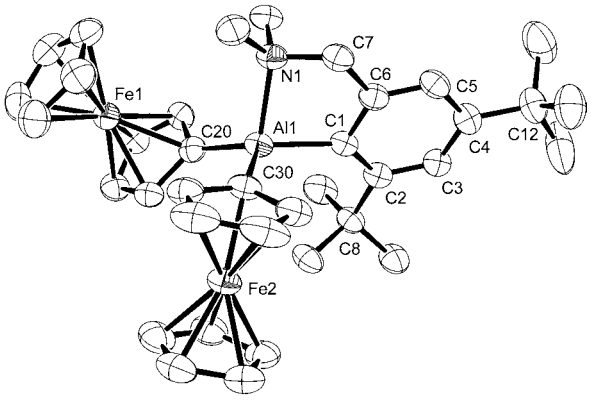

Figure 3. Molecular structure of **4a** with thermal ellipsoids at the 50% probability level. Hydrogen atoms and the solvent molecule C_6H_6 are omitted for clarity. Selected atom−atom distances [Å] and bond angles [°] for **4a**: Al1−C1 = 2.012(3), Al1−C20 = 1.966(4), Al1−C30 = 1.969(3), Al1−N1 = 2.038(3), Fe1−Al1 = 3.7250(11), Fe2−Al1 = 3.7746(10), C1−Al1−C20 = 124.08(14), C1−Al1−C30 = 114.03(14), C1−Al1−N1 = 86.87(12), C20−Al1−C30 = 114.06(14), N1−Al1−C20 = 111.05(13), N1−Al1−C30 = 99.85(13), Al1−C1−C2 = 137.8(2), Al1−C1−C6 = 106.0(2).

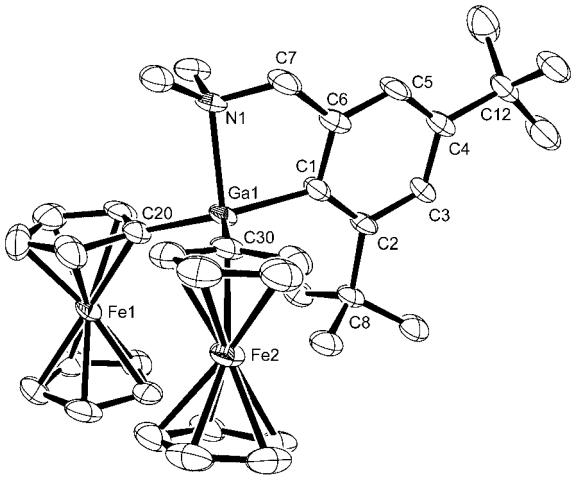

Figure 4. Molecular structure of **4b** with thermal ellipsoids at the 50% probability level. Hydrogen atoms are omitted for clarity. Selected atom−atom distances [Å] and bond angles [°] for **4b**: Ga1−C1 = 2.011(4), Ga1−C20 = 1.971(4), Ga1−C30 = 1.984(4), Ga1−N1 = 2.153(3), Fe1−Ga1 = 3.8107(7), Fe2−Ga1 = 3.7569(8), C1−Ga1−C20 = 129.04(17), C1−Ga1−C30 = 111.99(17), C1−Ga1−N1 = 84.11(15), C20−Ga1−C30 = 117.57(18), N1−Ga1−C20 = 98.27(15), N1−Ga1−C30 = 99.75(15), Ga1−C1−C2 = 133.7(3), Ga1−C1−C6 = 108.6(3).

only slightly lifted out of the plane of the base (**4a**: 0.322(5) Å; **4b**: 0.135(2) Å). The C−E bond lengths are very similar in both compounds and, as expected, respective bonds are slightly longer in the case of gallium. The Ga−N donor bond in **4b** of 2.153(3) Å is significantly longer than the Al−N bond of 2.038(3) Å in **4a**. Similar differences are known from comparable species and are a testament to the higher Lewis acidity toward N-donors of aluminum compared to respective gallium compounds.[26]

In ^{1}H and ^{13}C NMR spectra, compounds **4a** and **4b** each show similar signal patterns. For example, in the typical Cp range of ^{1}H NMR spectra, the presence of five peaks in a 5:1:1:1:1 intensity ratio shows the equivalency of both ferrocenyl moieties; i.e., **4a** and **4b** are C_s symmetric on the NMR time scale (500 MHz; C_6D_6 solutions). Two different conformers of the homologues **4a** and **4b** were found in the solid state (Figure 3 and 4), which probably indicates that the barrier of rotation of the ferrocenyl moieties is low. Therefore, the finding of C_s symmetric species in solution is expected.

DFT Calculations. The distortion in [1]metallacyclophanes is commonly described by a set of angles (Figure 5). The most

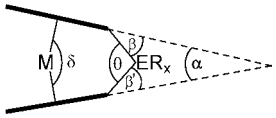

Figure 5. Common angles to describe distortions in [1]-metallacyclophanes.

discussed angle to illustrate the distortion in a [1]-metallacyclophane is the angle between the two least-squares planes defined by the carbon atoms of the Cp rings (tilt angle α). Despite the large number of [1]ferrocenophanes only four [1]ruthenocenophanes are known to date [ER_x: Zr-$(C_5H_4t\text{Bu})_2$,[27] SnMes*$_2$,[27] Al(Me_2Ntsi),[12] and Ga-(Me_2Ntsi)[12]]. Comparing respective [1]ferrocenophanes with [1]ruthenocenophanes shows that the α angle increases from iron to ruthenium in the range of 4.4−6.0° (Zr,[27,28] Sn,[27,29] Al,[10,12] and Ga,[10,12]). One expects that an increase of the tilt of both Cp moieties is accompanied by an increase in strain, which is expected to result in species of higher reactivity.[2a,30] On that basis, it is very surprising that the galla[1]-ruthenocenophane **3b** is isolable, whereas its iron counterpart **2b** is not. Furthermore, tilt angles α for alumina- and galla[1]ferrocenophanes **2a** and **2b**, respectively, should be similar to those of other aluminum- and gallium-bridged [1]ferrocenophanes, which were found in the range of 15−16°.[10,31] Tilt angles in that range are not expected to impose enough strain that alone can explain the high reactivity observed for **2a** and **2b**. We set out to further our understanding of these surprising experimental results with DFT calculations. In particular, we were interested in evaluating if different reactivities can be traced back to differences in ground-state geometries, e.g., if the Mamx ligand introduces different amounts of strain on [1]ferrocenophanes than on [1]ruthenocenophanes. Second, we wanted to find out if the *ortho*-*t*Bu has an influence on the structures and the reactivity of the strained sandwich compounds. This intention originated in the observation that the *ortho*-*t*Bu in the metallopolymers $\mathbf{2a_n}$ and $\mathbf{2b_n}$ is a very sensitive probe of the tacticity; e.g., for $\mathbf{2b_n}$ pentads of the polymer could be resolved by ^{1}H NMR spectroscopy.[19] This unusually high sensitivity could be caused by an intimate contact between this group and ferrocene repeating moieties.

In a first set of calculations, geometries of known aluminum and gallium-bridged [1]ferrocenophanes (**6a**, **6b**) and [1]-ruthenocenophanes (**7a**, **7b**) were optimized and compared to molecular structures known from single crystal X-ray analyses (Chart 3 and Table 3). Geometry optimizations were done on a BP86/TZ2P level using the ADF suite of programs.[32] This method has been shown to reproduce structures of metallocenophanes successfully.[8b,33] Calculated and experimentally determined angles to describe distortions in [1]-metallacyclophanes are compiled in Table 3 showing good to excellent agreement. For example, the tilt angles α calculated

dx.doi.org/10.1021/ja3019274 | J. Am. Chem. Soc. 2012, 134, 7924−7936

Chart 3. Overview of [1]Ferrocenophanes and [1]Ruthenocenophanes

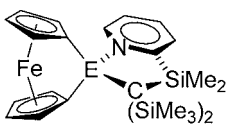

6a (Al)
6b (Ga)

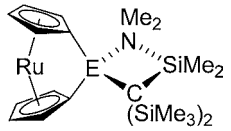

7a (Al)
7b (Ga)

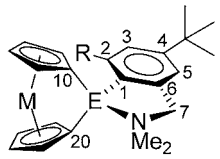

	R = *t*Bu		R = H	
	Fe	Ru	Fe	Ru
Al	**2a**	**3a**	**2a^H**	**3a^H**
Ga	**2b**	**3b**	**2b^H**	**3b^H**

for the two [1]ferrocenophanes **6a** and **6b** agree with measured values within three estimated standard deviations, if one considers molecule **6b** with the higher α angle of 16.40(20)° (Table 3). For the aluminum-bridged [1]ruthenocenophane **7a**, the calculated α angle is 0.92° below, whereas for the gallium species **7b**, it is 1.81° above the measured value. For the [1]ferrocenophane **6b** two independent molecules had been found in the asymmetric unit with tilt angles α of 15.44(21) and 16.40(20)°, respectively.[31] This example illustrates that the deviation of ±1° can be caused by packing effects in the solid state. In addition, for known aluminum- and gallium-bridged [1]metallacyclophanes, aluminum species always exhibit smaller tilt angles than their gallium counterparts. For example, for [1]chromarenophanes the difference is 1.4° [Al: 11.81(9)°; Ga: 13.24(13)°],[10c] whereas for [1]molybdarenophanes, equipped with the same bridging moiety E(Me_2Ntsi) (Chart 2), the difference amounts to 3.0° [Al: 18.28(17)°; Ga: 21.24(10)°].[11] The measured difference of only 0.6° for [1]ruthenocenophanes **7a** and **7b** is surprisingly small [Al: 20.31(19)°; Ga: 20.91(19)°].[12] Based on the difference of 3.0° found for [1]molybdarenophanes, the calculated difference of 3.3° for **7a** and **7b** matches with the expectation better than the experimentally determined difference of only 0.6°.

In a second series of calculations, geometries of the known [1]ferrocenophanes, **2a** and **2b**, and [1]ruthenocenophanes, **3a** and **3b**, were optimized on the same level of theory that was successfully applied to **6a,b** and **7a,b**. As mentioned before, we intended to find out if the *ortho*-*t*Bu group has an influence on the structure and, potentially, on the reactivity of strained sandwich compounds. In order to evaluate the structural influence of the *ortho*-*t*Bu group, molecular structures of the four unknown species **2a^H**, **2b^H**, **3a^H**, and **3b^H** (Chart 3), where this group was replaced by a H atom, were calculated as well. Table 4 compiles all calculated structural parameters commonly used to describe [1]metallocenophanes (Figure 5). The tilt angle α varies between 12.36 and 15.80° for [1]-ferrocenophanes and between 18.29° and 22.90° for [1]-ruthenocenophanes. Comparing respective aluminum and gallium compounds, the gallium species show α angles that are larger by 2.58 and 2.92° for ferrocenophanes and by 3.53 and 3.79° for ruthenocenophanes. The tilt angle α is not very sensitive toward the *ortho*-*t*Bu group. If this group is absent, the angle α decreases only by 0.86 and 0.52° for ferrocenophanes and by 1.08 and 0.82° for ruthenocenophanes.

Table 4. Calculated Angles [°] for [1]Ferrocenophanes and [1]Ruthenocenophanes[a]

	M/E/R	α	β/β'	θ	δ
2a	Fe/Al/*t*Bu	13.22	40.61/40.89	95.13	169.73
2a^H	Fe/Al/H	12.36	43.06/43.33	97.45	170.16
2b	Fe/Ga/*t*Bu	15.80	38.06/37.78	91.59	167.30
2b^H	Fe/Ga/H	15.28	39.57/39.30	93.28	167.49
3a	Ru/Al/*t*Bu	19.37	41.90/41.46	102.80	166.44
3a^H	Ru/Al/H	18.29	44.80/44.47	105.41	166.90
3b	Ru/Ga/*t*Bu	22.90	37.49/37.90	98.06	163.23
3b^H	Ru/Ga/H	22.08	39.88/40.21	100.47	163.66

[a]See Figure 5 and Chart 3.

Table 5 compiles bond lengths around aluminum and gallium, respectively, of all calculated species (see Chart 3 for numbering of atoms). Data in Table 5 reveals that all bonds around the bridging element are slightly lengthened in species equipped with the *ortho*-*t*Bu group. The average overall difference for all four types of bonds (E−N, E−C1, E−C10, and E−C20) is just 0.017 Å, with the smallest average difference found for E−N bonds (0.006 Å) and the largest found for E−C1 (0.033 Å). Even though the absolute values are small, they hint at a tension caused by the presence of the *t*Bu in the ortho position. However, the most pronounced structural effect can be seen as a change of the orientation of the bridging moiety with respect to the sandwich unit. The M−E−C1 angle decreases between 8.08 (**2b** to **2b^H**) and 12.73° (**3a** to **3a^H**) (see Table 5), whereas at the same time the tilt of the aromatic ring relative to the sandwich moiety changes the torsion angle M−E−C1−C2 in the range of 5.26 and 6.98° (Table 5 and Chart 3). It appears that as the *t*Bu group gets removed, the aromatic ligand moves toward the freed-up space. This main structural change is also illustrated in Figure 6 with the galla[1]ruthenocenophanes **3b** and **3b^H** as examples. The

Table 3. Comparison of Calculated and Measured Angles [°] of the Known [1]Ferrocenophanes 6a,b and [1]Ruthenocenophanes 7a,b[a]

	α		β/β'		θ		δ	
	calc.	exp.[b]	calc.	exp.[b]	calc.	exp.[b]	calc.	exp.[b]
6a	14.02	14.9(3)	39.96/40.05	39.6(4)/40.5(4)[c]	94.22	94.7(2)	169.02	167.9(3)
6b[d]	16.17	15.44(21)[d]	37.38/37.52	38.3(3)/39.0(2)[d]	90.95	92.68(13)[d]	166.91	166.96(17)[d]
		16.40(20)		38.5(3)/37.6(2)		92.22(13)		166.31(16)
7a	19.39	20.31(19)	41.48/41.21	39.9(4)/40.6(4)	102.63	101.3(2)	166.26	165.2(2)
7b	22.72	20.91(19)	37.63/38.01	38.6(2)/38.6(3)	98.30	98.42(13)	163.33	163.71(15)

[a]See Figure 5 and Chart 3. [b]Experimental data taken from refs 10a (**6a**), 31 (**6b**), and 12 (**7a,b**). [c]Published value of 43.1° has been recalculated. [d]Two independent molecules were found in the asymmetric unit of **6b**.[31]

dx.doi.org/10.1021/ja3019274 | J. Am. Chem. Soc. 2012, 134, 7924−7936

Table 5. Calculated Bond Lengths [Å] and Angles [°] for [1]Ferrocenophanes and [1]Ruthenocenophanes[a]

	M/E/R	E−N	E−C1	E−C10	E−C20	M−E−C1	M−E−C1−C2	$pl^{M,C10,C20}$−C1[b]
2a	Fe/Al/*t*Bu	2.078	2.014	2.015	2.005	153.31	−27.62	1.042
2a^H	Fe/Al/H	2.071	1.980	1.997	1.990	141.88	−22.36	1.603
2b	Fe/Ga/*t*Bu	2.193	2.013	2.025	2.036	157.24	−25.66	0.906
2b^H	Fe/Ga/H	2.184	1.981	2.012	2.019	149.16	−19.95	1.291
3a	Ru/Al/*t*Bu	2.070	2.011	2.033	2.044	151.26	−30.42	1.174
3a^H	Ru/Al/H	2.065	1.979	2.021	2.029	138.53	−23.44	1.770
3b	Ru/Ga/*t*Bu	2.181	2.013	2.049	2.062	155.60	−28.01	1.003
3b^H	Ru/Ga/H	2.177	1.980	2.035	2.043	144.88	−21.33	1.518

[a]See Chart 3. [b]Distance of C1 from the plane defined by M, C10, and C20 (see Figure 6).

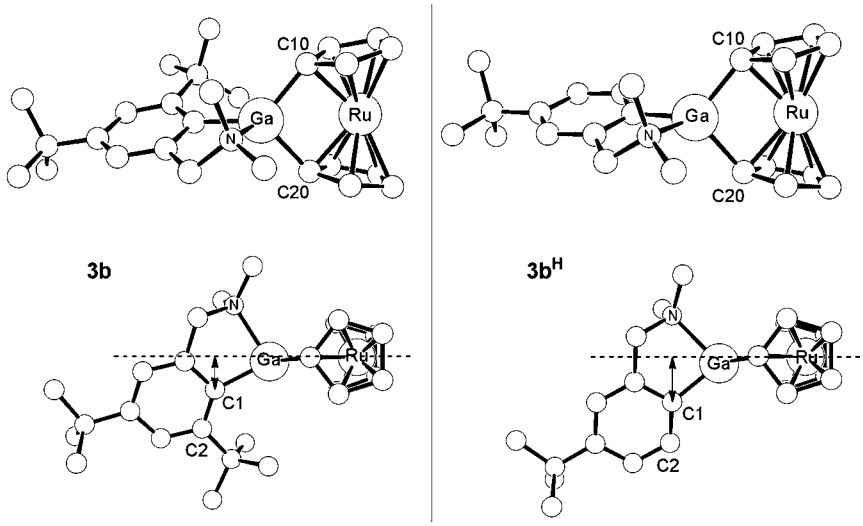

Figure 6. Optimized geometries of the galla[1]ruthenocenophanes **3b** and **3b^H**. Hydrogen atoms are omitted for clarity. The double-headed arrow illustrates the distance of C1 of 1.003 (**3b**) and 1.518 Å (**3b^H**) from the plane Ru−C10−C20 (dotted line) (see Tables 4 and 5).

species without the *ortho*-*t*Bu group (**3b^H**) shows a significant larger distance between C1 and the plane Ru−C10−C20 (double headed arrow in Figure 6). All other respective distances are listed in Table 5.

Thermochemistry. We intended to evaluate the effect of the *ortho*-*t*Bu group on the reactivity of strained species. So far, only structural effects of the *ortho*-*t*Bu group have been described showing that the removal of the *t*Bu group results in a relaxation of the remaining ligand toward the opened-up space. We wanted to quantify the energy change associated with these structural changes, and consequently, the amount of strain in species with and without the *t*Bu group needed to be calculated. Intrinsic strain of a compound can be best described by the enthalpy of a reaction where the strained species is transformed into an unstrained species. As shown in Scheme 3, the hydrogenation reaction (eq 1) was chosen as the chemically simplest possibility to release the strain. Table 6 provides an overview of the calculated thermodynamic values.

Scheme 3. Hydrogenation Reaction to Evaluate Strain in [1]Metallacyclophanes

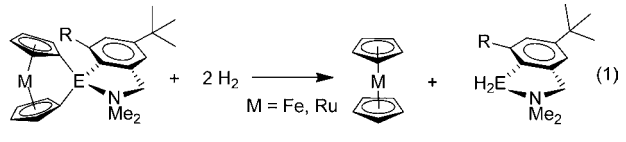

E \ R	*t*Bu	H
Al	**8a**	**8a^H**
Ga	**8b**	**8b^H**

Table 6. Thermodynamic Data [kcal/mol] of the Hydrogenolysis Reaction (eq 1 in Scheme 3)

	M/E/R	ΔE	ΔH^{298K}	ΔG^{298K}
2a	Fe/Al/*t*Bu	−29.31	−18.97	−13.47
2a^H	Fe/Al/H	−25.83	−12.64	−9.922
2b	Fe/Ga/*t*Bu	−40.41	−28.54	−24.54
2b^H	Fe/Ga/H	−37.59	−23.74	−21.13
3a	Ru/Al/*t*Bu	−32.31	−22.45	−15.67
3a^H	Ru/Al/H	−28.63	−16.52	−10.56
3b	Ru/Ga/*t*Bu	−44.87	−33.38	−28.02
3b^H	Ru/Ga/H	−41.83	−28.35	−24.15

The hydrogenation reaction (eq 1) is not isodesmic, and therefore, calculated enthalpies are not equal to the intrinsic strain of respective metallocenophanes. The calculated thermodynamic values are a mix of the release of strain of the sandwich species and the loss and gain of energy associated with bond breakage and formation. However, if one compares the hydrogenation of a *t*Bu containing species (e.g., **2a**) with that of the respective metallocenophane where the *t*Bu group is lacking (e.g., **2a^H**), then the difference in the calculated thermodynamic values ($\Delta\Delta E$, $\Delta\Delta H$, and $\Delta\Delta G$) provide a measure of the effect of the *ortho*-*t*Bu group. From the listed $\Delta\Delta E$, $\Delta\Delta H$, and $\Delta\Delta G$ values in Table 7 one can see that all species with the *ortho*-*t*Bu group (**2a**, **2b**, **3a**, and **3b**) are more

dx.doi.org/10.1021/ja3019274 | J. Am. Chem. Soc. 2012, 134, 7924−7936

Table 7. Effect of the *ortho*-*t*Bu Group on the Hydrogenolysis Reaction (eq 1 in Scheme 3)[a]

M/E	$\Delta\Delta E$	$\Delta\Delta H^{298K}$	$\Delta\Delta G^{298K}$
Fe/Al	−3.48	−6.33	−3.55
Fe/Ga	−2.82	−4.80	−3.41
Ru/Al	−3.68	−5.94	−5.10
Ru/Ga	−3.86	−5.03	−3.86

[a]Values in kcal/mol. Negative values indicate that species with R = *t*Bu result in a larger release of energy.

strained than their slimmer counterparts (**2a**^{H}, **2b**^{H}, **3a**^{H}, and **3b**^{H}).

The calculated increases of enthalpies are between −4.80 and −6.33 kcal/mol (Table 7) which raises the question of whether these increases are significant. The best experimental measurement of the strain present in a metallocenophane is the enthalpy of the thermal ROP. The text book example of a strained sandwich compound, dimethylsila[1]ferrocenophane, was found to release ca. 19 kcal/mol (ΔH^{ROP}).[34] With respect to this value, the average increase of strain caused by the *ortho*-*t*Bu group of 5.5 kcal/mol is indeed substantial.

As mentioned above, the hydrogenation reaction has the disadvantage that the absolute values of calculated thermodynamic data are meaningless. Therefore, an isodesmic reaction was sought and reaction 2 was investigated (Scheme 4).

Scheme 4. Isodesmic Reaction to Evaluate Strain in [1]Metallacyclophanes

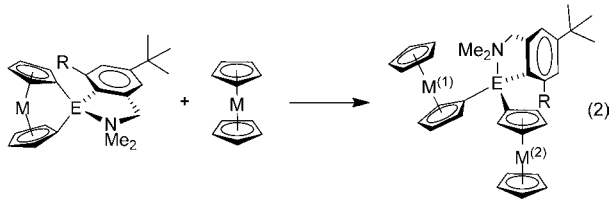

	R = *t*Bu		R = H	
	Fe	Ru	Fe	Ru
Al	**4a**	**5a**	**4a**^{H}	**5a**^{H}
Ga	**4b**	**5b**	**4b**^{H}	**5b**^{H}

Reaction 2 results in bis(metallocenyl) species of type **4** or **5**, which can be envisioned as model compounds for the respective polymers obtained by ROP of strained [1]-metallocenophanes. Hence, the calculated heat of eq 2 should be a very good approximation of the exothermy of a ROP.

As discussed above, the bis(ferrocenyl) compounds **4a** and **4b** crystallized with different orientations of the ferrocenyl moieties (Figures 3 and 4). These two different conformers, I and II, are illustrated in Figure 7. Two series of geometry calculations have been performed: one with starting geometries like that of **4a** (conformer I) and one with starting geometries like that of **4b** (conformer II). In both series convergence was obtained, but the size and floppiness of the bis(metallocenyl) compounds precluded reliable frequency calculations. Except for the two ferrocenophanes **4a**^{H} and **4b**^{H}, conformer I is energetically preferred over conformer II (ΔE = 1.63 (**4a**), 0.56 (**4b**), 2.80 (**5a**), 3.07 (**5b**), 1.69 (**5a**^{H}), and 0.54 (**5b**^{H}) kcal/mol). For the aluminum compound **4a**^{H}, both conformers are of equal energy (ΔE = −0.08 kcal/mol), whereas in the case of the gallium analogue **4b**^{H}, conformer II is slightly more stable (ΔE = −0.61 kcal/mol).

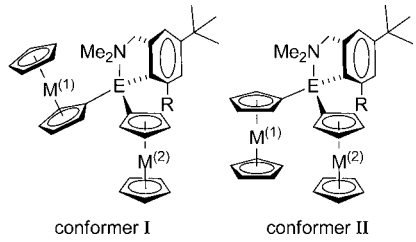

Figure 7. Conformers I and II of bis(metallocenyl) species **4a**, **4b**, **5a**, **5b**, **4a**^{H}, **4b**^{H}, **5a**^{H}, and **5b**^{H}. See Tables S14−S29 for Cartesian coordinates of all 16 optimized geometries.

Because the size and floppiness of the bis(metallocenyl) compounds precluded reliable frequency calculations, only ΔE values could be determined for the isodesmic reaction 2 (Table 8). As indicated in Scheme 4, only conformer I was taken into account. All eight reactions are exothermic with ΔE values varying for ferrocenophanes between −16.73 and −21.27 kcal/mol and for ruthenocenes between −22.13 and −26.74 kcal/mol. Surprisingly, species with the *ortho*-*t*Bu group seemed to be either slightly less than (**2a** and **2b**) or similarly strained (**3a** and **3b**) as their slimmer counterparts **2a**^{H}, **2b**^{H}, **3a**^{H}, and **3b**^{H} (see $\Delta\Delta E$ values in Table 8). These unexpected results contrast the results of the hydrogenation reaction (eq 1) discussed above.

Table 8. Comparison of Thermodynamic Data [kcal/mol] of the Isodesmic Reaction (eq 2 in Scheme 4)

	M/E/R	ΔE		M/E/R	ΔE	$\Delta\Delta E$[a]
2a	Fe/Al/*t*Bu	−16.73	**2a**^{H}	Fe/Al/H	−17.74	1.01
2b	Fe/Ga/*t*Bu	−19.94	**2b**^{H}	Fe/Ga/H	−21.27	1.33
3a	Ru/Al/*t*Bu	−22.13	**3a**^{H}	Ru/Al/H	−22.32	0.19
3b	Ru/Ga/*t*Bu	−26.74	**3b**^{H}	Ru/Ga/H	−26.74	0.00

[a]Positive values indicate that species with R = H result in a larger release of energy.

A close inspection of the structures of conformer I of bis(metallocenyl) species **4** and **5** uncovers that the species with the *ortho*-*t*Bu group are structurally distorted compared to those without the *ortho*-*t*Bu group. Table 9 provides an overview of selected structural parameters of products of type **4** and **5**; Figure 8 shows the calculated geometries of the two aluminum species **4a** and **4a**^{H}. The comparison of measured and calculated structural parameters for **4a** (Table 9) illustrates the excellent match of theory and experiment. Only the Al−N bond cannot be reproduced well. The most striking effect of the *ortho*-*t*Bu on the structures of the bis(metallocenyl) compounds **4** and **5** can be best illustrated by a comparison of E−M distances (E = Al or Ga; M = Fe or Ru; Figure 8 and Table 9). For example, by changing from species **4a** to species **4a**^{H} one Al−Fe distance is shortened by only 0.052 Å (E−Fe(1)), whereas the other Al−Fe distance decreases strongly by 0.249 Å from 3.791 to 3.542 Å (E−Fe(2); Figure 8). This structural difference can also be seen by a comparison of angles between E, the *ipso*-C^{Cp} atom, and the centroid of that Cp ring (E−C_{ipso}−centr(1) and E−C_{ipso}−centr(2) in Table 9). For the *t*Bu-containing species the centroid−M(2)−centroid axis of the metallocenyl unit is tilted away from the element E, whereas for the slimmer species the respective axis is tilted in the opposite direction, toward the element E. This difference in the direction of the tilting is illustrated with angle τ which is defined in Figure 9 as the centroid(2)−E−C_{ipso} angle. Starting from

dx.doi.org/10.1021/ja3019274 | J. Am. Chem. Soc. 2012, 134, 7924−7936

Table 9. Calculated Structural Parameters [Å and °] of Conformer I of Bis(metallocenyl) Species of Type 4 and 5 (Scheme 4)[a]

	E−M(1)	E−M(2)	E−N	E−C_{ipso}(1)	E−C_{ipso}(2)	E−$C_{arom.}$	E−C_{ipso}−centr(1)	E−C_{ipso}−centr(2)	τ[c]
4a	3.792 [3.7250(11)]	3.791 [3.7746(10)]	2.109 [2.038(3)]	1.985 [1.966(4)]	1.981 [1.969(3)]	2.022 [2.012(3)]	171.26 [174.55]	171.65 [170.89]	171.65 [170.89]
4a^H	3.740	3.542	2.126	1.978	1.972	1.995	173.40	174.08[b]	185.92
4b	3.803	3.775	2.247	1.989	1.986	2.029	170.95	172.52	172.52
4b^H	3.757	3.590	2.275	1.979	1.970	1.998	172.71	177.02[b]	182.98
5a	3.892	3.881	2.106	1.988	1.985	2.016	171.99	172.87	172.87
5a^H	3.883	3.673	2.120	1.982	1.976	1.993	172.44	176.27[b]	183.73
5b	3.892	3.863	2.235	1.989	1.985	2.024	171.68	173.37	173.37
5b^H	3.897	3.700	2.255	1.981	1.974	1.995	171.14	178.39[b]	181.61

[a]Measured values of **4a** are given in square brackets. [b]Sandwich unit is tilted toward the element E and not away from the element like in **4a**, **4b**, **5a**, and **5b** as shown in Figure 9 (see text for discussion). [c]Angle τ is defined as in Figure 9 (see text for discussion).

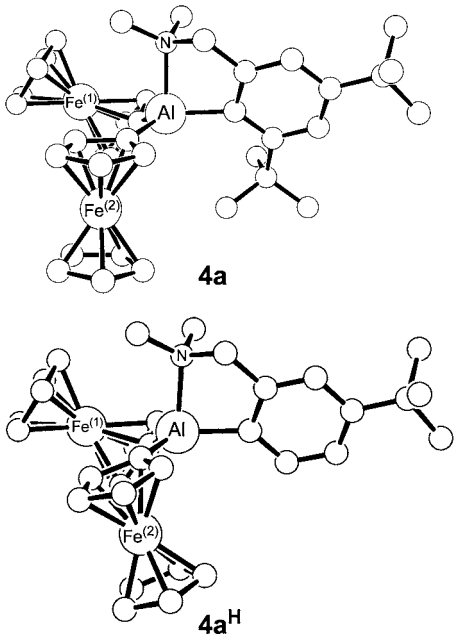

Figure 8. Optimized geometries of **4b** and **4b^H**. Hydrogen atoms are omitted for clarity.

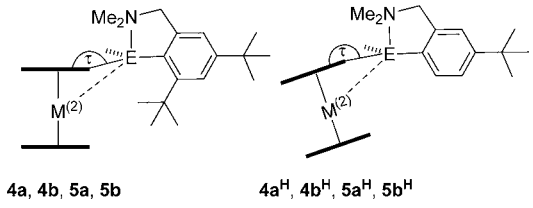

Figure 9. Illustration of the effect of the *ortho*-*t*Bu group on the tilting direction of the metallocenyl moiety of $M^{(2)}$ (angle τ) and the associated change in E−$M^{(2)}$ distances. See Scheme 4 and Table 9 and text for discussion.

centroid(2), τ is smaller than 180° for the *ortho*-*t*Bu containing compounds and larger than 180° for the less bulkier species **2a^H**, **2b^H**, **3a^H**, and **3b^H** (Figure 9). The differences for angle τ for respective pairs range from 8.24° (**5b**/**5b^H**) to 14.27° (**4a**/**4a^H**) (see Table 9 and Figure 9). These differences show the space requirements of the *ortho*-*t*Bu group: the *t*Bu group points toward the metallocenyl unit M(2) and forces it to be bent away (τ < 180°). Removal of the *t*Bu group let the metallocenyl unit M(2) relax, which goes hand-in-hand with the decrease of E−M(2) distances as discussed above (Figure 8 and 9; Table 9). The degree of bending is less pronounced for ruthenium compounds than for iron species, with differences of respective E−M(2) distances of 0.249 (Al) and 0.185 (Ga) for ferrocene species and 0.208 (Al) and 0.163 (Ga) for ruthenocene compounds (Table 9). Presumably, the larger spacing between the two Cp rings in ruthenocenes reduces the steric congestion compared with that in ferrocenes.

The structural differences caused by the *ortho*-*t*Bu group in species of type **4** and **5** clearly show that molecules equipped with the *ortho*-*t*Bu group are strained compared to their less bulky counterparts **4a^H**, **4b^H**, **5a^H**, and **5b^H**. Hence, the isodesmic reaction 2 (Scheme 4) does not provide a good measurement of the effect of the *ortho*-*t*Bu group on the strain in metallocenophanes.

SUMMARY AND CONCLUSION

Common salt metathesis reactions between dilithio sandwich species and aluminum or gallium dichlorides (Mamx)ECl_2 (**1a**, **1b**) resulted in the two [1]ferrocenophanes **2a** and **2b**[19] and the two new [1]ruthenocenophanes **3a** and **3b**. In contrast to the large number of known [1]ferrocenophanes, their ruthenium counterparts are rare and **3a** and **3b** being only the fifth and the sixth species of this type known to date. Surprisingly, only the gallium-bridged [1]ruthenocenophane **3b** was isolable, whereas the other three strained sandwich compounds polymerized under the conditions of their formation reactions. However, the isolable **3b** is similarly reactive as the other strained species and polymerizes if left in solution. Polymer **3b$_n$** can be obtained with a significantly increased molecular weight through Pt^0-catalyzed ROP employing Karstedt's catalyst. Overall, polymers **2a$_n$**, **2b$_n$**,[19] **3a$_n$**, and **3b$_n$** were prepared with molecular weights between 8.07 and 106 kDa (Table 2). DFT calculations have been performed to shed some light on the unexpected high reactivity of these new strained sandwich species. In particular, the role of the *t*Bu group in the ortho position at the bulky Mamx ligand (Chart 2) was investigated by comparing species equipped with the Mamx ligand (**2a**, **2b**, **3a**, and **3b**) with those where the *ortho*-*t*Bu group had been eliminated (**2a^H**, **2b^H**, **3a^H**, and **3b^H**; Chart 3). These investigations uncovered that the average increase in strain caused by the *ortho*-*t*Bu group is 5.5 kcal/mol ($\Delta\Delta H^{298K}$; Table 7). This is a significant increase of strain, if compared with measured enthalpy of polymerization of dimethylsila[1]-ferrocenophane (ΔH^{ROP} = 19 kcal/mol).[34] Structurally, the effect of the *ortho*-*t*Bu group can mainly be seen in a tilting of the Mamx ligand toward the side, while tilt angles α do not change significantly (Figure 6). To the best of our knowledge,

dx.doi.org/10.1021/ja3019274 | J. Am. Chem. Soc. 2012, 134, 7924−7936

such an unusual effect has never been observed in strained sandwich compounds before. This unusual effect of a *t*Bu group was deduced from a hydrogenolysis of the strained sandwich compounds, which had the disadvantage of being a non-isodesmic reaction (Scheme 3). The isodesmic reaction of aluminum- or gallium-bridged [1]metallocenophanes with ferrocene or ruthenocene (Scheme 4) could not be used to extract the strain present in [1]ferrocenophanes (**2a**, **2b**) or [1]ruthenocenophanes (**3a**, **3b**). The *ortho*-*t*Bu group in the resulting bis(metallocenyl) species **4a**, **4b**, **5a**, and **5b** sterically interacts with one of the metallocenyl units (Figure 9). The resulting structural distortion was confirmed by comparing the calculated and measured molecular structures of the aluminum compound **4a** (Figure 3 and Table 9). Bis(metallocenyl) species of type **4** and **5** can be envisioned as the smallest representative cutout of metallopolymers and the isodesmic reaction 2 (Scheme 4) provides important information about the ROP of [1]metallocenophanes **2a**, **2b**, **3a**, and **3b**. Even though the *ortho*-*t*Bu group imposes additional strain on the starting metallocenophanes, this effect cancels out in ROPs because the *ortho*-*t*Bu group imposes a similar strain on the resulting polymers.

We reported that the proton NMR signal of the *ortho*-*t*Bu group of polymer $\mathbf{2b_n}$ is split into 10 singlets,[19] revealing a random tacticity of the polymer. It was a surprise that the *ortho*-*t*Bu group was so sensitive toward the tacticity of the polymer and its signal could be resolved into the different pentads. Our new finding that the *ortho*-*t*Bu group in bis(metallocenyl) species sterically interacts with the sandwich moieties clearly reveals that similar interactions must be present in respective metallopolymers. We speculate that this steric repulsion causing the *ortho*-*t*Bu to act as such an unusually sensitive probe of the tacticity.

The initial intention of the DFT calculations was to improve our understanding of the high reactivity of aluminum- and gallium-bridged [1]metallocenophanes. We were puzzled that only one [1]ruthenocenophane (**3b**) was isolable, whereas compounds **2a**, **2b**, and **3a** were not isolable. However, theory did not reveal any unexpected differences between the geometries of [1]ferrocenophanes and [1]ruthenocenophanes. We could not find any clear evidence for the unexpected high reactivity of the prepared strained sandwich compounds, and hence, we can only conclude that kinetics governs the reactivity of these species. Unfortunately, the mechanism of the ROP of the aluminum- and gallium-bridged compounds is still unknown. It seems likely that small amounts of dilithioferrocene in reaction mixtures of the salt metathesis reaction act as an anionic initiator for ROP (Scheme 1), but several attempts to trap anions by addition of excess of Me_3SiCl did not result in a measurable effect on the polymerization reaction.

EXPERIMENTAL SECTION

General Procedures. All syntheses were carried out using standard Schlenk and glovebox techniques (N_2 as inert gas), unless noted differently. Toluene, Et_2O, thf, hexane, and CH_2Cl_2 were dried using an MBraun Solvent Purification System and stored under nitrogen over 3 Å molecular sieves. Degassed C_6H_6 and MeOH were dried over 3 Å molecular sieves under N_2. All solvents for NMR spectroscopy were degassed prior to use and stored under N_2 over 3 Å molecular sieves. ^{1}H and ^{13}C NMR spectra were recorded on a Bruker 500 MHz Avance NMR spectrometer at 25 °C in C_6D_6 and CD_2Cl_2, respectively (^{1}H at 500.28 MHz; ^{13}C at 125.80 MHz). ^{1}H chemical shifts were referenced to the residual protons of the deuterated solvents (δ 7.15 for C_6D_6 and 5.32 for CD_2Cl_2); ^{13}C chemical shifts were referenced to the C_6D_6 signal at δ 128.00 and the CD_2Cl_2 signal at δ 54.00. Carbon atoms directly bound to group 13 elements in **1a**, **3b**, and **4a** were not detected in respective ^{13}C NMR spectra. UV−visible spectra were measured on a Varian Cary 50 UV−visible spectrophotometer. Mass spectra were measured on a VG 70SE and are reported in the form *m*/*z* (rel intens) [M$^+$] where "*m*/*z*" is the mass observed, "rel intens" is intensity of the peak relative to the most intense peak and "M$^+$" is the molecular ion or fragment; only characteristic mass peaks are reported. For isotopic pattern, only the mass peak of the isotopoloque or isotope with the highest natural abundance is listed. Elemental analyses were performed on a Perkin-Elmer 2400 CHN Elemental Analyzer using V_2O_5 to promote complete combustion.

Dynamic Light Scattering. Dynamic light scattering experiments were performed using a nano series Malvern zetasizer instrument equipped with a 633 nm red laser. Samples were filtered through 0.2 μm syringe PTFE filters before they were analyzed in 1 cm glass cuvettes at concentrations of 4.0, 3.0, 2.0, and 1.0 mg/mL in CH_2Cl_2 at 25 °C. The refractive index of the polymers was assumed to be 1.5. For each polymer, three samples were prepared at each concentration. Every sample was measured three times. Few measured R_h values stand out as being either far too small or far too large and were not included in the analysis. For poly(ferrocenyldimethylsilane) (PFS) the absolute molecular weights (M_w) in the range of 10 to 100 kDa and their radii of gyration (R_g) are known in literature.[25] Assuming that the polymers $\mathbf{2a_n}$, $\mathbf{3a_n}$, and $\mathbf{3b_n}$ are random coils in good solvents, measured R_h values were converted into R_g values using the factor $R_g/R_h = 2.05$[24] and the published relation between log(R_g) and log(M_w) for PFS[25] was used to calculate M_w for $\mathbf{2a_n}$, $\mathbf{3a_n}$, and $\mathbf{3b_n}$ (see SI for more details).

Chemicals. $AlCl_3$ (98%), $FeCp_2$ (98%), *n*BuLi (2.8 M in hexanes), platinum(0)-1,3-divinyl-1,1,3,3-tetramethyldisiloxane (Karstedt's catalyst; 2 wt % in xylene), and C_6D_6 (99.6 atom % D) were purchased from Sigma Aldrich; $AlCl_3$ was sublimed prior to use. $GaCl_3$ (Alfa Aesar; 99.999%) and tetramethylethylenediamine (Alfa Aesar; 99%) were purchased from VWR. $RuCl_3{\cdot}xH_2O$ (99%) was purchased from Precious Metals Online. CD_2Cl_2 (99.9 atom % D) was purchased from Cambridge Isotope Laboratories. The compounds $(LiC_5H_4)CpFe$,[35] $(LiC_5H_4)_2Fe{\cdot}2/3tmeda$,[36] $RuCp_2$,[37] $(LiC_5H_4)_2Ru{\cdot}tmeda$,[27] 6-$(Me_2NCH_2)$-2,4-$tBu_2C_6H_2$Br (MamxBr),[19] and (Mamx)$GaCl_2$ (**1b**)[19] were synthesized according to literature procedures.

Synthesis of {2,4-Di-*tert*-butyl-6-[(dimethylamino)methyl]-phenyl}dichloroalumane (1a). *n*BuLi (2.8 M in hexanes, 7.90 mL, 22.1 mmol) was added dropwise to a cold (−78 °C) solution of MamxBr (6.53 g, 20.0 mmol) in Et_2O (30 mL). The reaction mixture was stirred at −78 °C for 45 min and a cold (0 °C) solution of $AlCl_3$ (2.66 g, 20.0 mmol) in Et_2O (30 mL) was added dropwise. The resulting mixture was warmed up to r.t. and stirred for 16 h, resulting in a pale yellow solution with a colorless precipitate. After the solid was filtered off, the pale yellow solution was concentrated to approximately 20 mL, and analytically pure product **1a** was obtained as needle-shaped, colorless crystals at −22 °C (5.65 g, 82%). ^{1}H NMR (C_6D_6): δ 1.33 (s, 9H, *t*Bu-4), 1.59 (s, 9H, *t*Bu-2), 1.92 (s, 6H, NMe_2), 3.13 (s, 2H, CH_2), 6.74 (s, 1H, CH-5), 7.58 (s, 1H, CH-3). ^{13}C NMR (C_6D_6): δ 31.60 [C($\underline{C}H_3)_3$-4], 32.84 [C($\underline{C}H_3)_3$-2], 34.87 [$\underline{C}(CH_3)_3$-4], 37.31 [$\underline{C}(CH_3)_3$-2], 45.57 (NMe_2), 65.66 (CH_2), 119.22 (C-5), 122.37 (C-3), 142.75 (C-6), 152.28 (C-4) 160.68 (C-2). EIMS (70 eV): *m*/*z* (%) 343 (14) [M$^+$], 328 (21) [M$^+$ - Me], 301 (48) [$C_{14}H_{22}AlCl_2N^+$], 292 (14) [$C_{16}H_{24}AlClN^+$], 247 (88) [$C_{17}H_{29}N^+$], 246 (57) [$C_{17}H_{28}N^+$], 203 (55) [$C_{15}H_{23}^+$], 190 (24) [$C_{14}H_{22}^+$], 189 (18) [$C_{14}H_{21}^+$], 187 (30) [$C_{14}H_{19}^+$], 148 (61) [$C_{11}H_{16}^+$], 147 (15) [$C_{11}H_{15}^+$], 146 (12) [$C_{11}H_{14}^+$], 133 (100) [$C_{10}H_{13}^+$], 131 (16) [$C_{10}H_{11}^+$], 91 (13) [$C_7H_7^+$], 58 (75) [$C_4H_{10}^+$], 57 (25) [$C_4H_9^+$]. Anal. Calcd for $C_{17}H_{28}Cl_2AlN$ (344.30): C, 59.30; H, 7.84; N, 4.07. Found: C, 59.39; H, 7.55; N, 4.07.

Identification of {2,4-Di-*tert*-butyl-6-[(dimethylamino)-methyl]phenyl}alumina[1]ferrocenophane (2a). Product **2a** is an intermediate in the preparation of polymer $\mathbf{2a_n}$ (see below) and can be identified via ^{1}H NMR spectroscopy. All attempts to isolate pure **2a** resulted in the isolation of polymer $\mathbf{2a_n}$. ^{1}H NMR (C_6D_6; taken from

dx.doi.org/10.1021/ja3019274 | J. Am. Chem. Soc. 2012, 134, 7924−7936

an aliquot of the reaction mixture after 30 min): δ 1.42 (s, 9H, *t*Bu-4), 1.71 (s, 9H, *t*Bu-2), 2.09 (s, 6H, NMe_2), 3.41 (s, 2H, CH_2), 3.85 (pst, 2H, CH-α), 4.51 (pst, 2H, CH-α), 4.70 (pst, 2H, CH-β), 4.72 (pst, 2H, CH-β), 6.87 (s, 1H, CH-5), 7.64 (s, 1H, CH-3).

Attempted Isolations of [1]Metallocenophanes 2a, 2b, and 3a. As soon as the [1]metallocenophane was detected by ^{1}H NMR spectroscopy (approximately 15−20 min after mixing the solution/slurry of the respective group 13 element dichloride and the dilithiometallocene), quick filtration was performed to remove LiCl. Following are the descriptions of our attempts to isolate [1]-metallocenophanes from the respective filtrate: (1) The filtrated was kept at −80 °C for several (7−30) days without any precipitate or crystals forming. The solution was warmed up to r.t. and ^{1}H NMR measurement from the solution revealed the presence of the [1]metallocenophane as well as respective polymeric product. (2) In many attempts, the filtrate was concentrated to variable degrees (approximately 2/3, 1/2, 1/3, 1/4) under reduced pressure. Different attempts were made to isolate [1]metallocenophane from these concentrated solutions: (a) A concentrated solution was kept at −22 °C or −80 °C for several (3−14) days, resulting in precipitates that were isolated and found to be polymeric product (^{1}H NMR spectroscopy). (b) A concentrated solution was added to well stirred hexane (approximately 3−4 times the volume of the concentrated solution) with the formation of precipitate which was isolated as polymeric material. (c) An open vial containing the concentrated solution was placed in a larger vial filled with hexane and the larger vial was closed to allow diffusion of one solvent into the other. The setup was left at r.t. or at −30 °C for several (3−14) days which gave precipitates that were again identified as polymers.

Synthesis of Poly(ferrocenylalumane) 2a$_n$. A solution of **1a** (0.797 g, 2.31 mmol) in Et_2O (65 mL) was added dropwise to a slurry of $(LiC_5H_4)_2Fe{\cdot}2/3$tmeda (0.639 g, 2.32 mmol) in Et_2O (40 mL) at r.t. The resulting reaction mixture was stirred for 4 h and then left unstirred for 16 h, resulting in a red gelatinous material. All volatiles were removed under vacuum, yielding a red paste. The crude product was extracted with benzene (50 mL) and the benzene solution was concentrated to approximately 10 mL. The concentrated benzene solution was added dropwise to hexane (60 mL) with vigorous stirring, yielding an orange precipitate with a red solution. The precipitate (0.438 g) was filtered off and dried under vacuum. For further purification, the orange solid was dissolved in benzene (15 mL) and added dropwise to MeOH (60 mL) with vigorous stirring, resulting in an orange precipitate and a pale yellow solution. The precipitate was filtered off and dried under vacuum to give **2a$_n$** (0.391 g, 37%). UV/vis: λ_{max} = 475 nm, ε = 0.29 mL (mg cm)$^{-1}$. ^{1}H NMR (C_6D_6): δ 1.40 (br. s, 9 H, *t*Bu-4), 1.86 (br. s with shoulders at 1.77, 9 H, *t*Bu-2), 1.97 (br. s, 6 H, NMe_2), 3.39 (br. s with shoulder at 3.43, 2 H, CH_2), 4.26, 4.33, 4.42 (3 br. s, 4H, CH-α), 4.76 (br. s, 4H, CH-β), 6.90 (br. s, 1 H, CH-3), 7.64 (br. s, 1 H, CH-5). ^{13}C NMR (C_6D_6): δ 31.90 [C($\underline{C}H_3)_3$-4], 33.79 [C($\underline{C}H_3)_3$-2], 34.71 [$\underline{C}(CH_3)_3$-4], 37.37 [$\underline{C}(CH_3)_3$-2], 45.73 (NMe_2), 67.21 (CH_2), 71.55, 72.87, 76.47, 76.60, 76.78 (C_5H_4), 118.91 (C-5), 121.67 (C-3), 142.41 (C-1), 144.49 (C-6), 149.77 (C-4), 160.75 (C-2).

Identification of {2,4-Di-*tert*-butyl-6-[(dimethylamino)-methyl]phenyl}alumina[1]ruthenocenophane (3a). Product **3a** is an intermediate in the preparation of polymer **3a$_n$** (see below) and can be identified via ^{1}H NMR spectroscopy. All attempts to isolate pure **3a** resulted in the isolation of polymer **3a$_n$**. ^{1}H NMR (C_6D_6; taken from an aliquot of the reaction mixture after 30 min): δ 1.40 (s, 9H, *t*Bu-4), 1.60 (s, 9H, *t*Bu-2), 1.97 (s, 6H, NMe_2), 3.42 (s, 2H, CH_2), 4.02 (pst, 2H, CH-α), 4.65 (pst, 2H, CH-α), 5.30 (pst, 2H, CH-β), 5.34 (pst, 2H, CH-β), 6.86 (s, 1H, CH-5), 7.61 (s, 1H, CH-3).

Synthesis of Poly(ruthenocenylalumane) 3a$_n$. A solution of **1a** (0.575 g, 1.67 mmol) in toluene (20 mL) was added dropwise to a slurry of $(LiC_5H_4)_2Ru{\cdot}$tmeda (0.600 g, 1.67 mmol) in toluene (15 mL) at r.t. The resulting reaction mixture was stirred for 4 h and then left unstirred for 16 h, resulting in a yellow solution with a colorless precipitate. The solid was filtered off and the yellow solution was concentrated to approximately 8 mL. The concentrated toluene solution was added dropwise to hexane (30 mL) with vigorous stirring, yielding in a pale yellow precipitate with a yellow solution. The precipitate (0.416 g) was filtered off and dried under vacuum. For further purification, the pale yellow solid was dissolved in 1:1 mixture of toluene/Et_2O (10 mL) and added dropwise to MeOH (30 mL) with vigorous stirring, resulting in an off-white precipitate and a pale yellow solution. The precipitate was filtered off and dried under vacuum to give **3a$_n$** (0.361 g, 43%). UV/vis: λ_{max} = 341 nm, ε = 0.29 mL (mg cm)$^{-1}$. ^{1}H NMR (CD_2Cl_2): δ 1.32 (br. s, 18 H, *t*Bu-2 and *t*Bu-4), 2.37 (br. s with shoulders at 2.36, 2.38 and 2.41, 6 H, NMe_2), 3.66 (br. s with shoulder at 3.68, 2 H, CH_2), 4.35, 4.37, 4.41, 4.43, 4.48, 4.49, 4.59, 4.60 (3 br. s with shoulders, 8H, CH-α and CH-β), 6.92 (br. s with shoulder at 6.93, 1 H, CH-5), 7.38 (br. s, 1 H, CH-3). ^{13}C NMR (CD_2Cl_2): δ 31.81,[C($\underline{C}H_3)_3$-4], 33.54 [C($\underline{C}H_3)_3$-2], 34.99 [$\underline{C}(CH_3)_3$-4], 37.26 [$\underline{C}(CH_3)_3$-2], 46.36 (NMe_2), 67.85 (CH_2), 70.47, 70.59, 70.95, 71.79, 72.06, 73.35, 77.58, 77.78, 77.96, 79.52 (C_5H_4), 119.79 (C-5), 122.01 (C-3), 142.25, 142.52, 142.91 (C-1), 143.34 (C-6), 149.40 (C-4), 158.65 (C-2).

Synthesis of {2,4-Di-*tert*-butyl-6-[(dimethylamino)methyl]-phenyl}galla[1]ruthenocenophane (3b). A solution of **1b** (1.51 g, 3.90 mmol) in toluene (35 mL) was added dropwise to a slurry of $(LiC_5H_4)_2Ru{\cdot}$tmeda (1.42 g, 3.95 mmol) in toluene (20 mL). The reaction mixture was stirred at r.t. for 2 h, resulting in a yellow solution with a colorless precipitate. After the solid was filtered off, the yellow solution was concentrated to approximately 15 mL, yielding a cloudy mixture which was added dropwise to hexane (35 mL) with vigorous stirring, yielding a yellow solution with a pale yellow precipitate. The reaction flask was kept at −30 °C for 16 h to complete the precipitation. The precipitate was filtered off and dried under vacuum to give product **3b** (1.06 g, 50%). Attempt to crystallize **3b**: A saturated solution of **3b** was prepared in different organic solvents (Et_2O, thf, toluene, and benzene). Following are the attempts to crystallize **3b** from the saturated solutions: (1) The solutions were kept for several (7−14) days at low temperature (−22 °C for Et_2O, thf, and toluene solutions and 6 °C for benzene solutions). (2) An open vial containing the saturated solution was placed in a larger vial filled with hexane and the larger vial was closed to allow diffusion of one solvent into the other. The setup was left at r.t. or at lower temperatures (+6 or −30 °C) for several (7−14) days. Crystals were never obtained; however, these attempts gave precipitates that were identified as polymers by ^{1}H NMR spectroscopy.

^{1}H NMR (C_6D_6): δ 1.39 (s, 9H, *t*Bu-4), 1.55 (s, 9H, *t*Bu-2), 1.95 (s, 6H, NMe_2), 3.30 (s, 2H, CH_2), 4.05 (pst, 2H, CH-α of Cp), 4.59 (pst, 2H, CH-α of Cp), 5.34 (pst, 2H, CH-β of Cp), 5.36 (pst, 2H, CH-β of Cp), 6.89 (s, 1H, CH-5), 7.62 (s, 1H, CH-3). ^{13}C NMR (C_6D_6): δ 31.67 [C($\underline{C}H_3)_3$-4], 32.92 [C($\underline{C}H_3)_3$-2], 34.81 [$\underline{C}(CH_3)_3$-4], 36.49 [$\underline{C}(CH_3)_3$-2], 46.55 (NMe_2), 67.65 (CH_2), 76.32, 78.41, 78.81, 79.34 (C_5H_4), 119.46 (C-5), 121.26 (C-3), 142.16 (C-6), 150.46 (C-4) 158.38 (C-2). Anal. Calcd for $C_{27}H_{36}GaNRu$ (545.37): C, 59.46; H, 6.65; N, 2.57. Found: C, 58.59; H, 6.95; N, 2.45.

Synthesis of Poly(ruthenocenylgallane) 3b$_n$ through Transition-Metal-Catalyzed ROP. Platinum(0)-1,3-divinyl-1,1,3,3-tetramethyldisiloxane (2 wt % Pt in xylene, 0.557 mL, 0.025 mmol) was added dropwise to a solution of **3b** (0.275 g, 0.504 mmol) in toluene (5 mL) at r.t. The reaction mixture was stirred at r.t. for 16 h, yielding a brown solution which was concentrated to ca. 2 mL. The concentrated solution was added to hexane (30 mL) with vigorous stirring, yielding a brown solution with pale yellow precipitate which was filtered off and dried under vacuum. For further purification, the pale yellow solid was dissolved in toluene (3 mL) and added dropwise to MeOH (30 mL) with vigorous stirring, resulting in an off-white precipitate and a pale yellow solution. The precipitate was filtered off and dried under vacuum to give **3b$_n$** (0.141 g, 56%). UV/vis: λ_{max} = 347 nm, ε = 0.32 mL (mg cm)$^{-1}$. ^{1}H NMR (C_6D_6): δ 1.37 (br. s, 9 H, *t*Bu-4), 1.58 (br. s with shoulders at 1.56,1.63, 1.65 and 1.67, 9 H, *t*Bu-2), 2.10 (br. s with shoulders at 2.05, 2.08, 2.18 and 2.19, 6 H, NMe_2), 3.42 (br. s with shoulder at 3.30, 2 H, CH_2), 4.65 (br. s with shoulders at 4.56, 4.60 and 4.73, 4H, CH-α), 4.93 (br. s with shoulders at 4.90 and 5.01, 4H, CH-β), 6.98 (br. s with shoulder at 6.95, 1 H, CH-5), 7.62 (br. s, 1 H, CH-3). ^{13}C NMR (C_6D_6): δ 31.44 [C($\underline{C}H_3)_3$-4], 33.28 [C($\underline{C}H_3)_3$-2], 34.38 [$\underline{C}(CH_3)_3$-4], 36.89 [$\underline{C}(CH_3)_3$-2], 45.23,

dx.doi.org/10.1021/ja3019274 | J. Am. Chem. Soc. 2012, 134, 7924−7936

45.27 (NMe_2), 67.09 (CH_2), 70.06, 70.28, 70.56, 70.65, 71.61, 71.85, 71.95, 72.80, 73.15, 77.47, 78.86, 79.11 (C_5H_4), 118.98 (C-5), 121.70 (C-3), 142.50 (C-1), 143.30 (C-6), 149.16 (C-4), 158.93 (C-2).

Synthesis of Poly(ruthenocenylgallane) $3b_n$ through Uncontrolled ROP. A solution of **1b** (3.75 g, 9.69 mmol) in toluene (55 mL) was added dropwise to a slurry of $(LiC_5H_4)_2Ru{\cdot}$tmeda (3.51 g, 9.77 mmol) in toluene (30 mL) at r.t. The resulting reaction mixture was stirred for 16 h, resulting in a yellow solution with white precipitate. The solid was filtered off and the yellow solution was concentrated to ca. 20 mL. The concentrated solution was added dropwise to hexane (100 mL) with vigorous stirring, yielding a pale yellow precipitate with a yellow solution. The precipitate (0.438 g) was filtered off and dried under vacuum. For further purification, the pale yellow solid was dissolved in toluene (25 mL) and added dropwise to MeOH (100 mL) with vigorous stirring, resulting in an off-white precipitate and a pale yellow solution. The precipitate was filtered off and dried under vacuum to give product $3b_n$ (2.53 g, 52%).

Synthesis of {2,4-Di-*tert*-butyl-6-[(dimethylamino)methyl]-phenyl}bis(ferrocenyl)alumane (4a). A solution of **1a** (0.690 g, 2.00 mmol) in Et_2O (40 mL) was added dropwise to a slurry of $(LiC_5H_4)CpFe$ (0.967 g, 5.04 mmol) in Et_2O (30 mL) at r.t. The reaction mixture was stirred for 16 h, resulting in a red solution with an orange precipitate. After the solid was filtered off, all volatiles were removed under vacuum, yielding a red paste as the crude product which was washed with hexane (3 × 50 mL), resulting in an orange solid. The solid was dissolved in Et_2O (30 mL), the Et_2O solution was concentrated to approximately to 10 mL and added to hexane (50 mL) with vigorous stirring. The resulting orange precipitate was filtered off and dried under vacuum, yielding **4a** as an orange powder (0.657 g, 51%). ^{1}H NMR (C_6D_6): δ 1.38 (s, 9H, *t*Bu-4), 1.71 (s, 9H, *t*Bu-2), 1.83 (s, 6H, NMe_2), 3.28 (s, 2H, CH_2), 4.11, 4.27, 4.35, 4.41 (pst, 8H, C_5H_4), 4.23 (s, 10H, C_5H_5), 6.89 (s, 1H, CH-5), 7.66 (s, 1H, CH-3). ^{13}C NMR (C_6D_6): δ 31.69 [$C(\underline{C}H_3)_3$-4], 33.66 [$C(\underline{C}H_3)_3$-2], 34.72 [$\underline{C}(CH_3)_3$-4], 37.29 [$\underline{C}(CH_3)_3$-2], 45.55 (NMe_2), 67.07 (CH_2), 68.34 (C_5H_5), 70.83, 70.90, 76.52, 76.91 (C_5H_4), 118.86 (C-5), 121.62 (C-3), 144.29 (C-6), 150.15 (C-4) 160.78 (C-2). EIMS (70 eV): *m*/*z* (%) 643 (100) [M^+], 458 (12) [M^+ - $C_{10}H_9Fe$], 186 (17) [$C_{10}H_{10}Fe^+$]. Anal. Calcd for $C_{37}H_{46}AlFe_2N$ (643.44): C, 69.07; H, 7.21; N, 2.18. Found: C, 69.84; H, 7.05; N, 2.01.

Synthesis of {2,4-Di-*tert*-butyl-6-[(dimethylamino)methyl]-phenyl}bis(ferrocenyl)gallane (4b). A solution of **1b** (1.06 g, 2.02 mmol) in Et_2O (30 mL) was added dropwise to a slurry of $(LiC_5H_4)CpFe$ (0.967 g, 5.53 mmol) in Et_2O (30 mL) at r.t. The reaction mixture was stirred for 16 h, resulting in a red solution with an orange precipitate. After the solid was filtered off, all volatiles were removed under vacuum, yielding a red paste as the crude product which was dissolved in thf (10 mL). Pure product **4b** (0.685 g, 49%) was obtained in form of red-orange crystals from this thf solution at −22 °C. ^{1}H NMR (C_6D_6): δ 1.37 (s, 9H, *t*Bu-4), 1.71 (s, 9H, *t*Bu-2), 1.73 (s, 6H, NMe_2), 3.20 (s, 2H, CH_2), 4.06, 4.30, 4.31, 4.39 (pst, 8H, C_5H_4), 4.27 (s, 10H, C_5H_5), 6.93 (s, 1H, CH-5), 7.69 (s, 1H, CH-3). ^{13}C NMR (C_6D_6): δ 31.70 [$C(\underline{C}H_3)_3$-4], 33.49 [$C(\underline{C}H_3)_3$-2], 34.68 [$\underline{C}(CH_3)_3$-4], 37.04 [$\underline{C}(CH_3)_3$-2], 45.39 (NMe_2), 66.95 (CH_2), 68.45 (C_5H_5), 70.27, 70.33, 75.40, 75.78, 76.76 (C_5H_4), 119.45 (C-5), 122.00 (C-3), 142.42 (C-1), 143.65 (C-6), 149.67 (C-4) 159.02 (C-2). EIMS (70 eV): *m*/*z* (%) 685 (14) [M^+], 535 (100) [$C_{30}H_{36}FeGaN^+$], 186 (96) [$C_{10}H_{10}Fe^+$]. Anal. Calcd for $C_{37}H_{46}GaFe_2N$ (686.18): C, 64.76; H, 6.76; N, 2.04. Found: C, 64.48; H, 6.76; N, 1.98.

Crystal Structure Determination. Single crystals of **1b**, **4a**·$1/2C_6H_6$ and **4b** were coated with Paratone-N oil, mounted using a Micromount (*MiTeGen* - Microtechnologies for Structural Genomics), and frozen in the cold stream of the Oxford cryojet attached to the diffractometer. Crystal data were collected at −100 °C on a Bruker-AXS Proteum R Smart 6000 3-Circle diffractometer using monochromated Cu Kα radiation (λ = 1.54184 Å). An initial orientation matrix and cell was determined from ω scans, and the X-ray data were measured using φ and ω scans.[38] Data reduction was performed using *SAINT* included in the *APEX2* software package.[38] A multiscan absorption correction was applied (*SADABS*).[39]

Structures were solved by direct methods (*SIR-2004*)[40] and refined by full-matrix least-squares methods on F^2 with *SHELX-97*.[39] Unless otherwise stated, the non-hydrogen atoms were refined anisotropically; hydrogen atoms were included at geometrically idealized positions but not refined. The isotropic thermal parameters of the hydrogen atoms were fixed at 1.2 times that of the preceding carbon atom. For the structure **4b** diffraction data from two crystals with similar size were combined in order to obtain enough data for solving the structure. It appeared that the crystals decomposed over time upon exposure to X-ray radiation.

Computational Details. Theoretical calculations were carried out using the Amsterdam density functional package (version ADF2010.02).[32] The Slater-type orbital (STO) basis sets were of triple-ζ quality augmented with a two polarization functions (ADF basis TZ2P). Core electrons were frozen (C, N 1s; Al, Si, Fe 2p; Ru 3d) in our model of the electronic configuration for each atom. Relativistic effects were included by virtue of the zero order regular approximation (ZORA).[41] The local density approximation (LDA) by Vosko, Wilk, and Nusair (VWN)[42] was used together with the exchange correlation corrections of Becke[43] and Perdew[44] (BP86).[43,44] Tight optimization conditions were used for the monomer series of compounds **2**, **3**, **6**, **7**, **8**, MCp_2, and H_2. Frequency calculations were used to confirm minima and provide thermodynamic information. Some compounds showed small imaginary frequencies corresponding to barrierless rotation of cyclopentadienyl rings or *t*Bu groups. The large size and number of conformers of the bis(metallocenyl) species of type **4** and **5** necessitated TZP basis sets and more relaxed optimization conditions for these molecules. The resulting optimized structures were then subjected to single point calculations with TZ2P basis sets to obtain consistent values for the reaction 2 (Scheme 4).

■ ASSOCIATED CONTENT

Ⓢ Supporting Information

Crystallographic data for **1b**, **4a**, and **4b** in CIF file format; DLS data for $2a_n$, $3a_n$, and $3b_n$ (Tables S1−S5; Figures S1−S4); NMR spectra of **1a**, **2a**, $2a_n$, **3a**, $3a_n$, **3b**, $3b_n$, **4a**, and **4b** (Figures S5−S22); Cartesian coordinates for all calculated species (Tables S6−S39). This material is available free of charge via the Internet at http://pubs.acs.org.

■ AUTHOR INFORMATION

Corresponding Author

jens.mueller@usask.ca

Notes

The authors declare no competing financial interest.

■ ACKNOWLEDGMENTS

We thank the Natural Sciences and Engineering Research Council of Canada (NSERC Discovery Grant, J.M.) for support. We thank the Canada Foundation for Innovation (CFI) and the government of Saskatchewan for funding of the X-ray and NMR facilities in the Saskatchewan Structural Sciences Centre (SSSC). We thank Prof. Ildiko Badea (University of Saskatchewan, College of Pharmacy and Nutrition) for making the DLS instrument available for our studies.

■ REFERENCES

(1) Foucher, D. A.; Tang, B.-Z.; Manners, I. *J. Am. Chem. Soc.* **1992**, *114*, 6246−6248.

(2) (a) Herbert, D. E.; Mayer, U. F. J.; Manners, I. *Angew. Chem., Int. Ed.* **2007**, *46*, 5060−5081. (b) Tamm, M. *Chem. Commun.* **2008**, 3089−3100. (c) Braunschweig, H.; Kupfer, T. *Acc. Chem. Res.* **2010**, *43*, 455−465.

(3) Bellas, V.; Rehahn, M. *Angew. Chem., Int. Ed.* **2007**, *46*, 5082−5104.

(4) Selected Reviews: (a) Manners, I. *Science* **2001**, *294*, 1664−1666. (b) Manners, I. *Synthetic Metal-Containing Polymers*; Wiley-VCH: Weinheim, Germany, 2004. (c) Marin, V.; Holder, E.; Hoogenboom, R.; Schubert, U. S. *Chem. Soc. Rev.* **2007**, *36*, 618−635. (d) Whittell, G. R.; Manners, I. *Adv. Mater.* **2007**, *19*, 3439−3468. (e) Williams, K. A.; Boydston, A. J.; Bielawski, C. W. *Chem. Soc. Rev.* **2007**, *36*, 729−744. (f) Eloi, J. C.; Chabanne, L.; Whittell, G. R.; Manners, I. *Mater. Today* **2008**, *11*, 28−36. (g) Hempenius, M. A.; Cirmi, C.; Lo Savio, F.; Song, J.; Vancso, G. J. *Macromol. Rapid Commun.* **2010**, *31*, 772−783. (h) Wong, W. Y.; Harvey, P. D. *Macromol. Rapid Commun.* **2010**, *31*, 671−713. (i) Krüger, R. A.; Baumgartner, T. *J. Chem. Soc., Dalton Trans.* **2010**, *39*, 5759−5767. (j) Manners, I. *J. Organomet. Chem.* **2011**, *696*, 1146−1149. (k) Whittell, G. R.; Hager, M. D.; Schubert, U. S.; Manners, I. *Nat. Mater.* **2011**, *10*, 176−188.

(5) (a) Rulkens, R.; Ni, Y. Z.; Manners, I. *J. Am. Chem. Soc.* **1994**, *116*, 12121−12122. (b) Ni, Y. Z.; Rulkens, R.; Manners, I. *J. Am. Chem. Soc.* **1996**, *118*, 4102−4114.

(6) (a) Wang, X. S.; Guerin, G.; Wang, H.; Wang, Y. S.; Manners, I.; Winnik, M. A. *Science* **2007**, *317*, 644−647. (b) Gädt, T.; Ieong, N. S.; Cambridge, G.; Winnik, M. A.; Manners, I. *Nat. Mater.* **2009**, *8*, 144−150. (c) Gilroy, J. B.; Gädt, T.; Whittell, G. R.; Chabanne, L.; Mitchels, J. M.; Richardson, R. M.; Winnik, M. A.; Manners, I. *Nature Chem.* **2010**, *2*, 566−570. (d) Presa Soto, A.; Gilroy, J. B.; Winnik, M. A.; Manners, I. *Angew. Chem., Int. Ed.* **2010**, *49*, 8220−8223. (e) Gädt, T.; Schacher, F. H.; McGrath, N.; Winnik, M. A.; Manners, I. *Macromolecules* **2011**, *44*, 3777−3786. (f) Gilroy, J. B.; Patra, S. K.; Mitchels, J. M.; Winnik, M. A.; Manners, I. *Angew. Chem., Int. Ed.* **2011**, *50*, 5851−5855. (g) He, F.; Gädt, T.; Manners, I.; Winnik, M. A. *J. Am. Chem. Soc.* **2011**, *133*, 9095−9103. (h) Patra, S. K.; Ahmed, R.; Whittell, G. R.; Lunn, D. J.; Dunphy, E. L.; Winnik, M. A.; Manners, I. *J. Am. Chem. Soc.* **2011**, *133*, 8842−8845.

(7) (a) Cheng, F.; Jäkle, F. *Polym. Chem.* **2011**, *2*, 2122−2132. (b) Jäkle, F. *Chem. Rev.* **2010**, *110*, 3985−4022.

(8) (a) Braunschweig, H.; Dirk, R.; Müller, M.; Nguyen, P.; Resendes, R.; Gates, D. P.; Manners, I. *Angew. Chem., Int. Ed.* **1997**, *36*, 2338−2340. (b) Berenbaum, A.; Braunschweig, H.; Dirk, R.; Englert, U.; Green, J. C.; Jäkle, F.; Lough, A. J.; Manners, I. *J. Am. Chem. Soc.* **2000**, *122*, 5765−5774.

(9) (a) Heilmann, J. B.; Qin, Y.; Jäkle, F.; Lerner, H. W.; Wagner, M. *Inorg. Chim. Acta* **2006**, *359*, 4802−4806. (b) Heilmann, J. B.; Scheibitz, M.; Qin, Y.; Sundararaman, A.; Jäkle, F.; Kretz, T.; Bolte, M.; Lerner, H. W.; Holthausen, M. C.; Wagner, M. *Angew. Chem., Int. Ed.* **2006**, *45*, 920−925. (c) Scheibitz, M.; Li, H. Y.; Schnorr, J.; Perucha, A. S.; Bolte, M.; Lerner, H. W.; Jäkle, F.; Wagner, M. *J. Am. Chem. Soc.* **2009**, *131*, 16319−16329.

(10) (a) Schachner, J. A.; Lund, C. L.; Quail, J. W.; Müller, J. *Organometallics* **2005**, *24*, 785−787. (b) Schachner, J. A.; Lund, C. L.; Quail, J. W.; Müller, J. *Organometallics* **2005**, *24*, 4483−4488. (c) Lund, C. L.; Schachner, J. A.; Quail, J. W.; Müller, J. *Organometallics* **2006**, *25*, 5817−5823.

(11) Lund, C. L.; Schachner, J. A.; Quail, J. W.; Müller, J. *J. Am. Chem. Soc.* **2007**, *129*, 9313−9320.

(12) Schachner, J. A.; Tockner, S.; Lund, C. L.; Quail, J. W.; Rehahn, M.; Müller, J. *Organometallics* **2007**, *26*, 4658−4662.

(13) (a) Braunschweig, H.; Burschka, C.; Clentsmith, G. K. B.; Kupfer, T.; Radacki, K. *Inorg. Chem.* **2005**, *44*, 4906−4908. (b) Schachner, J. A.; Orlowski, G. A.; Quail, J. W.; Kraatz, H.-B.; Müller, J. *Inorg. Chem.* **2006**, *45*, 454−459. (c) Lund, C. L.; Schachner, J. A.; Burgess, I. J.; Quail, J. W.; Schatte, G.; Müller, J. *Inorg. Chem.* **2008**, *47*, 5992−6000.

(14) Schachner, J. A.; Lund, C. L.; Burgess, I. J.; Quail, J. W.; Schatte, G.; Müller, J. *Organometallics* **2008**, *27*, 4703−4710.

(15) Mamx stands for methylaminomethyl-*m*-xylyl; see ref 16.

(16) Yoshifuji, M.; Kamijo, K.; Toyota, K. *Tetrahedron Lett.* **1994**, *35*, 3971−3974.

(17) (a) Yoshifuji, M.; Sangu, S.; Kamijo, K.; Toyota, K. *Chem. Ber.* **1996**, *129*, 1049−1055. (b) Kamijo, K.; Otoguro, A.; Toyota, K.; Yoshifuji, M. *Bull. Chem. Soc. Jpn.* **1999**, *72*, 1335−1342. (c) Kamijo, K.; Toyota, K.; Yoshifuji, M. *Chem. Lett.* **1999**, 567−568. (d) Kawasaki, S.; Fujita, T.; Toyota, K.; Yoshifuji, M. *Bull. Chem. Soc. Jpn.* **2005**, *78*, 1082−1090.

(18) (a) Schmidt, H.; Keitemeyer, S.; Neumann, B.; Stammler, H.-G.; Schoeller, W. W.; Jutzi, P. *Organometallics* **1998**, *17*, 2149−2151. (b) Jutzi, P.; Keitemeyer, S.; Neumann, B.; Stammler, H.-G. *Organometallics* **1999**, *18*, 4778−4784.

(19) Bagh, B.; Gilroy, J. B.; Staubitz, A.; Müller, J. *J. Am. Chem. Soc.* **2010**, *132*, 1794−1795.

(20) ortho refers to the position of the *t*Bu group with respect to gallium.

(21) Isom, H. S.; Cowley, A. H.; Decken, A.; Sissingh, F.; Corbelin, S.; Lagow, R. J. *Organometallics* **1995**, *14*, 2400−2406.

(22) Schumann, H.; Wassermann, B. C.; Schutte, S.; Heymer, B.; Nickel, S.; Seuss, T. D.; Wernik, S.; Demtschuk, J.; Girgsdies, F.; Weimann, R. *Z. Anorg. Allg. Chem.* **2000**, *626*, 2081−2095.

(23) Sometimes the difference between peaks for β-protons in ^{1}H NMR spectra is not measurable; see for example **2b**.

(24) Burchard, W. *Branched Polymers II* **1999**, *143*, 113−194.

(25) Massey, J. A.; Kulbaba, K.; Winnik, M. A.; Manners, I. *J. Polym. Sci., Part B: Polym. Phys.* **2000**, *38*, 3032−3041.

(26) See donor bond lengths in [1.1]ferrocenophanes[13a,b] (Al−N = 2.0748(14); Ga−N = 2.178(3) Å; bridging moieties Ar'E), [1.1]chromarenophanes[13c] (Al−N = 2.089(4); Ga−N = 2.192(2) Å; bridging units (*p*-*t*BuAr')E), or [1.1]molybdarenophanes[13c] (Al−N = 2.096(3); Ga−N = 2.207(3) Å; bridging units (*p*-*t*BuAr')E).

(27) Vogel, U.; Lough, A. J.; Manners, I. *Angew. Chem., Int. Ed.* **2004**, *43*, 3321−3325.

(28) Broussier, R.; Darold, A.; Gautheron, B.; Dromzee, Y.; Jeannin, Y. *Inorg. Chem.* **1990**, *29*, 1817−1822.

(29) Jäkle, F.; Rulkens, R.; Zech, G.; Foucher, D. A.; Lough, A. J.; Manners, I. *Chem.—Eur. J.* **1998**, *4*, 2117−2128.

(30) Green, J. C. *Chem. Soc. Rev.* **1998**, *27*, 263−271.

(31) Schachner, J. A.; Quail, J. W.; Müller, J. *Acta Crystallogr.* **2008**, *E64*, m517.

(32) (a) Baerends, E. J.; Ellis, D. E.; Ros, P. *Chem. Phys.* **1973**, *2*, 41−51. (b) Versluis, L.; Ziegler, T. *J. Chem. Phys.* **1988**, *88*, 322−328. (c) Velde, G. T.; Baerends, E. J. *J. Comput. Phys.* **1992**, *99*, 84−98. (d) Fonseca Guerra, C. F.; Snijders, J. G.; te Velde, G.; Baerends, E. J. *Theor. Chem. Acc.* **1998**, *99*, 391−403.

(33) (a) Matas, I.; Whittell, G. R.; Partridge, B. M.; Holland, J. P.; Haddow, M. F.; Green, J. C.; Manners, I. *J. Am. Chem. Soc.* **2010**, *132*, 13279−13289. (b) Masson, G.; Herbert, D. E.; Whittell, G. R.; Holland, J. P.; Lough, A. J.; Green, J. C.; Manners, I. *Angew. Chem., Int. Ed.* **2009**, *48*, 4961−4964. (c) Barlow, S.; Drewitt, M. J.; Dijkstra, T.; Green, J. C.; O'Hare, D.; Whittingham, C.; Wynn, H. H.; Gates, D. P.; Manners, I.; Nelson, J. M.; Pudelski, J. K. *Organometallics* **1998**, *17*, 2113−2120.

(34) ca. 80 kJ/mol were measured by DSC in the range of 120−170 °C; see ref 1.

(35) Bildstein, B.; Malaun, M.; Kopacka, H.; Wurst, K.; Mitterbock, M.; Ongania, K.-H.; Opromolla, G.; Zanello, P. *Organometallics* **1999**, *18*, 4325−4336.

(36) Butler, I. R.; Cullen, W. R.; Ni, J.; Rettig, S. J. *Organometallics* **1985**, *4*, 2196−2201.

(37) Liu, D.; Xie, F.; Zhang, W. *J. Org. Chem.* **2007**, *72*, 6992−6997.

(38) Bruker; Bruker AXS Inc.: Madison, WI, 2009.

(39) Sheldrick, G. M. *Acta Crystallogr., Sect. A* **2008**, *64*, 112−122.

(40) Burla, M. C.; Caliandro, R.; Camalli, M.; Carrozzini, B.; Cascarano, G. L.; De Caro, L.; Giacovazzo, C.; Polidori, G.; Spagna, R. *J. Appl. Crystallogr.* **2005**, *38*, 381−388.

(41) (a) Snijders, J. G.; Baerends, E. J.; Ros, P. *Mol. Phys.* **1979**, *38*, 1909−1929. (b) Ziegler, T.; Tschinke, V.; Baerends, E. J.; Snijders, J. G.; Ravenek, W. *J. Phys. Chem.* **1989**, *93*, 3050−3056. (c) van Lenthe, E.; Baerends, E. J.; Snijders, J. G. *J. Chem. Phys.* **1993**, *99*, 4597−4610.

(42) Vosko, S. H.; Wilk, L.; Nusair, M. *Can. J. Phys.* **1980**, *58*, 1200−1211.

(43) Becke, A. D. *Phys. Rev. A* **1988**, *38*, 3098−3100.

(44) Perdew, J. P. *Phys. Rev. B* **1986**, *33*, 8822−8824.